Efficient Acoustic Echo Cancellation With Reduced-Rank Adaptive Filtering Based on Selective Decimation and Adaptive Interpolation

Masahiro Yukawa, *Member, IEEE*, Rodrigo C. de Lamare, *Member, IEEE*, and Raimundo Sampaio-Neto

***Abstract*—This paper presents a new approach to efficient acoustic echo cancellation (AEC) based on reduced-rank adaptive filtering equipped with selective-decimation and adaptive interpolation. We propose a novel structure of an AEC scheme that jointly optimizes an interpolation filter, a decimation unit, and a reduced-rank filter. With a practical choice of parameters in AEC, the total computational complexity of the proposed reduced-rank scheme with the normalized least mean square (NLMS) algorithm is approximately half of that of the full-rank NLMS algorithm. We discuss the convergence properties of the proposed scheme and present a convergence condition. First, we examine the performance of the proposed scheme in a single-talk situation with an error-minimization criterion adopted in the decimation selection. Second, we investigate the potential of the proposed scheme in a double-talk situation by employing an ideal decimation selection. In addition to mean squared error (MSE) and power spectrum analysis of the echo estimation error, subjective assessments based on *absolute category rating* are performed, and the results demonstrate that the proposed structure provides significant improvements compared to the full-rank NLMS algorithm.**

***Index Terms*—Acoustic echo cancellation (AEC), reduced-rank adaptive filtering.**

I. Introduction

THE GOAL of this paper is to present a novel reduced-rank adaptive filtering scheme for an efficient acoustic echo cancellation (AEC) and to investigate its potential. The major advantages of reduced-rank adaptive filters are their faster convergence speed and better tracking performance over the full-rank ones when dealing with a large number of filter weights. Early reduced-rank methods and systems were based on principal components analysis, in which a computationally expensive singular value decomposition (SVD) to extract the signal subspace is required [1], [2]. A problem with early SVD-based methods is the selection of the adequate subspace for rank reduction, which was later solved with the cross-spectral (CS) method [3]. The multistage Wiener filter (MWF) has been developed in [4] and is based on orthogonal decompositions for computation of its parameters. The MWF was shown to exhibit better error-rate in DS/CDMA systems than the previously reported methods when the order of reduced-rank filter is small [5]. Another technique that resembles the MWF is the auxiliary-vector filtering (AVF) algorithm based on a finite number of auxiliary vectors orthogonal to each other and to the steering vector [6], [7]. The equivalence between the MWF and the AVF with orthogonal auxiliary vectors has been established in [8]. An AVF structure based on a sequence of (i.e., a infinite number of) auxiliary vectors, orthogonal to the steering vector but not necessarily to each other, has been proposed [9], which slightly outperforms the MWF at the cost of higher computational complexity. The major issue of these reduced-rank approaches is their high complexity $O(PN^2)$, where P stands for the dimension of the reduced-rank filter and N the dimension of the full-rank covariance matrix (or the steering vector) used to compute the subspace projection. A different class of flexible reduced-rank methods is based on the use of interpolated finite-impulse response (FIR) filters. A seminal work on interpolated FIR filters has been reported in [10], and the method has been applied to the AEC problem in [11]. Further improvements have been realized by means of a joint updating method of an interpolator and an FIR filter [12]. The interpolation-based approach is computationally simpler than the aforementioned approaches; however, its main drawback is that it is rank-limited, i.e., the designer cannot significantly reduce the filter rank since the system undergoes performance degradation.

In [13], preliminary results on a novel framework[1] for reduced-rank parameter estimation have been reported; the scheme is based on the joint optimization of an interpolation filter, a decimation unit, and a reduced-rank filter. In the scheme, the number of elements for estimation is substantially reduced, resulting in considerable computational savings and efficient tracking ability of dynamic signals. A unique feature of this reduced-rank scheme is that it does not rely on the full-rank covariance matrix (whose sample-average estimation may require a considerable amount of data) before projecting the received data onto a reduced-rank subspace. The key factor in this approach is the use of diversity techniques for the decimation-matrix-selection and the adaptive interpolator, which is inspired by diversity techniques developed in wireless communications.

Manuscript received May 8, 2007; revised December 5, 2007. The associate editor coordinating the review of this manuscript and approving it for publication was Prof. Sen M. Kuo.

M. Yukawa was with the Department of Electronics, University of York, York Y010 5DD, U.K. He is now with the Next Generation Mobile Communications Laboratory, CIPS, RIKEN, Saitama 351-0106, Japan (e-mail: myukawa@riken.jp).

R. C. de Lamare is with the Department of Electronics, University of York, York YO10 5DD, U.K. (e-mail: rcdl500@ohm.york.ac.uk).

R. Sampaio-Neto is with CETUC, Pontifical Catholic University of Rio de Janeiro (PUC-RIO), 22453-900 Gavea, Rio de Janeiro, RJ, Brazil (e-mail: raimundo@cetuc-puc-rio.br).

Digital Object Identifier 10.1109/TASL.2008.916059

[1]USPTO Application No. 11/427.471—Patent Pending.

1558-7916/$25.00 © 2008 IEEE

In this paper, we propose an efficient reduced-rank AEC scheme based on the framework reported in [13]. In the proposed scheme, the reduced-rank transformation is constructed by an adaptive interpolator and decimation matrix selected from parallel branches so that the output error is minimized, thus the transformation itself is time-varying. The total computational complexity of the proposed scheme is presented herein in terms of decimation factor, interpolation vector length, and *diversity factor* (i.e., the number of parallel branches). The number of adaptive elements in the reduced-rank filter is significantly reduced in comparison with the original full-rank filter. It is shown that a practical choice of those factors results in the complexity of $1.6N$, which is approximately twice more efficient than the normalized least mean square (NLMS) algorithm. Numerical examples demonstrate that an increase of diversity factor significantly improves the achievable mean squared error (MSE) in practical noisy environments. Specifically, the proposed reduced-rank AEC scheme with only three or four taps significantly outperforms a full-rank AEC structure with 1024 taps.

The remaining of the paper is organized as follows. Following brief descriptions of acoustic echo cancellation problem and reduced-rank adaptive filtering in Section II, the proposed echo canceling scheme is presented in Section III. In Section IV, we present the convergence properties of the scheme and discuss the convergence conditions of the algorithms. In Sections V and VI, numerical examples are presented in single-talk and double-talk cases, respectively, followed by the conclusion in Section VII.

II. Motivation and Problem Statement

To motivate the current study, we first present a problem formulation of acoustic echo cancellation. We then present a general idea of the reduced-rank adaptive filtering problem. Throughout the paper, $\mathbb{R}$ and $\mathbb{N}$ denote the sets of all real numbers and nonnegative integers, respectively.

A. AEC Problem

A basic model of an AEC system with a full-rank adaptive filter [14], [15] is illustrated in Fig. 1. We present the notation used throughout paper below [$(\cdot)^T$ stands for *transposition*].

- $k \in \mathbb{N}$: time index.
- $u_k \in \mathbb{R}$: far-end speech signal sample (input to $\boldsymbol{h}^*$).
- $w_k \in \mathbb{R}$: near-end speech signal sample.
- $n_k \in \mathbb{R}$: additive background noise sample.
- $\boldsymbol{h}^* \in \mathbb{R}^N (N \in \mathbb{N}^* := \mathbb{N} \setminus \{0\})$: echo impulse response.
- $d_k := \boldsymbol{u}_k^T \boldsymbol{h}^* + w_k + n_k \in \mathbb{R}$ with

$$\boldsymbol{u}_k := [u_k, u_{k-1}, \ldots, u_{k-N+1}]^T \in \mathbb{R}^N. \tag{1}$$

- $\boldsymbol{h}_k \in \mathbb{R}^N$: full-rank adaptive filter.

We let $u_k = 0, \forall k < 0$, so that the vector $\boldsymbol{u}_k$ can be defined for all $k \in \mathbb{N}$. As the distorted far-end speech signal $\boldsymbol{u}_k^T \boldsymbol{h}^*$ is transmitted back to the far-end talker's room with delay, it is referred to as acoustic echo. The goal of the echo cancellation is to remove (or cancel) the echo $\boldsymbol{u}_k^T \boldsymbol{h}^*$ from d_k by subtracting the output of adaptive (linear) filter $\boldsymbol{h}_k$, as $d_k - \boldsymbol{u}_k^T \boldsymbol{h}_k$. The adaptation of an echo canceler is mostly executed only when the near-end speech is not active, i.e., $w_k = 0$, since most approaches attempt to minimize (or suppress) the error between d_k and filter output (adaptation in $w_k \neq 0$ means that the adaptive filter cancels the near-end speech w_k together with the distorted far-end speech $\boldsymbol{u}_k^T \boldsymbol{h}^*$). Hence, in the following, we assume that $w_k = 0$ except for Section VI.

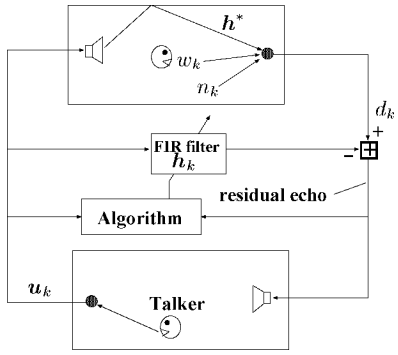

Fig. 1. Acoustic echo canceling scheme. u_k is the far-end talker's speech signal transmitted to the near-end talker's room at time k. d_k is the microphone signal generated by the near-end talker's signal w_k, the ambient noise n_k, and the distorted far-end talker's signal $\boldsymbol{u}_k^T \boldsymbol{h}^*$, where $\boldsymbol{h}^*$ is the impulse response of the echo path.

Because the required length of echo canceler is typically in the order of 1000 [16], it is strongly desired to establish an echo canceling scheme with low computational complexity, fast convergence, and effective tracking capability. To this end, we highlight the reduced-rank adaptive filtering in what follows.

B. Reduced-Rank Adaptive Filtering

The convergence and tracking speed of adaptive algorithm becomes in general slower when the number of taps N increases [14]. The aim of reduced-rank adaptive filtering is to attain faster convergence and better tracking capability by reducing the number of filter taps and extracting the most important features of the processed data. This dimensionality reduction is accomplished by a linear mapping from $\mathbb{R}^N$ to the feature-extracting space $\mathbb{R}^P$ with $\boldsymbol{S} \in \mathbb{R}^{N \times P}$, where $P < N$. The reduced-dimensionality input vector is denoted as

$$\widehat{\boldsymbol{u}}_k := \boldsymbol{S}^T \boldsymbol{u}_k \in \mathbb{R}^P, \ \forall k \in \mathbb{N}. \tag{2}$$

In the following, the P-dimensional vectors are denoted with a "hat." The P-dimensional vector $\widehat{\boldsymbol{u}}_k$ is the input to a tapped-delay line filter represented by $\widehat{\boldsymbol{h}}_k \in \mathbb{R}^P$. The filter output at time k is represented as

$$y_k := \widehat{\boldsymbol{h}}_k^T \widehat{\boldsymbol{u}}_k, \ \forall k \in \mathbb{N}. \tag{3}$$

The strategic and fundamental part in reduced-rank schemes is the design of the operator $\boldsymbol{S}$, which should be designed in an efficient (or optimal) way. In particular, the dimensionality reduction should be carried out such that the most important features of the input data are extracted. In the following section, we present an efficient and highly effective way to design $\boldsymbol{S}$ that changes dynamically in terms of k.

III. Proposed AEC Structure

The proposed AEC scheme consists of an adaptive interpolator, adaptive decimation procedure, and a reduced-rank adaptive FIR filter, as illustrated in Fig. 2. In Section III-A,

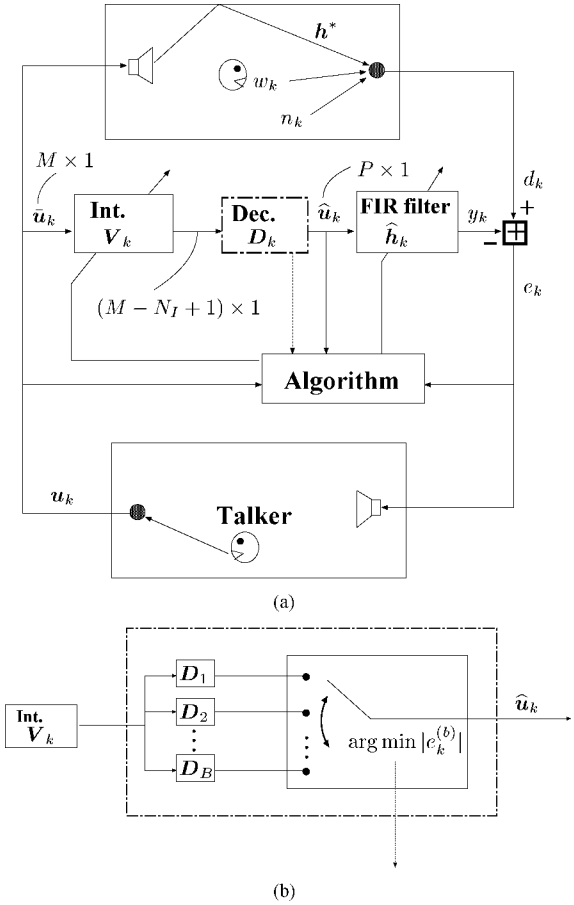

Fig. 2. (a) Acoustic echo canceler with the proposed structure and (b) an example of the decimation procedure. In (a), e_k denotes the residual echo, and the vector $\bar{\boldsymbol{u}}_k$ is compounded from the same signal as $\boldsymbol{u}_k$ with in general different length. In (b), $D_1, \ldots, D_B$ denote the decimation matrices, and $\widehat{\boldsymbol{u}}_k$ the decimated signal being the input to the FIR filter.

we describe the whole picture of the proposed scheme. In Section III-B, we present NLMS-based algorithms to update the interpolator and reduced-rank FIR filters, and an adaptive control of the decimation procedure.

A. Echo Canceler Structure

First of all, we introduce the parameters employed in the remaining of the paper.

- $N \in \mathbb{N}^* := \mathbb{N} \backslash \{0\}$: Length of the echo impulse response.
- $B \in \mathbb{N}^*$: the number of parallel decimation-branches (which we refer to as *diversity factor*).
- $D \in \mathbb{N}^*$: the decimation factor.
- $P := \lceil N/D \rceil$: the length (or rank) of the reduced-rank adaptive FIR filter, where $\lceil a \rceil$ denotes the smallest integer which is greater than or equal to $a \in \mathbb{R}$.
- $M := B + D(P-1) + N_I - 1$: the necessary length of data samples for the proposed scheme at each iteration (Note: $M \leq B + N + N_I - 2$).
- $N_I \in \mathbb{N}^*$: the length of the interpolator.

The notation u_k, w_k, n_k, d_k and $\boldsymbol{h}^*$ is the same as in Section II-A. For the sake of rank-reduction, we define two matrices as follows. The first one is the interpolation (Toeplitz) matrix

$$\boldsymbol{V}_k := \begin{bmatrix} \boldsymbol{v}_k & 0 & \cdots & 0 \\ & \boldsymbol{v}_k & & \vdots \\ \vdots & & \ddots & 0 \\ 0 & \cdots & 0 & \boldsymbol{v}_k \end{bmatrix} \in \mathbb{R}^{M \times (M - N_I + 1)}, \ \forall k \in \mathbb{N} \tag{4}$$

with the adaptive interpolation vector $\boldsymbol{v}_k \in \mathbb{R}^{N_I}$. The second one is the decimation matrix $\boldsymbol{D}_k$ selected from, $\forall b \in \{1, 2, \ldots, B\}$

$$\boldsymbol{D}_k^{(b)} := [\boldsymbol{\epsilon}_b \ \boldsymbol{\epsilon}_{b+D} \cdots \boldsymbol{\epsilon}_{b+D(P-1)}]^T \in \mathbb{R}^{P \times (M - N_I + 1)}, \ \forall k \in \mathbb{N}. \tag{5}$$

where $\boldsymbol{\epsilon}_i \in \mathbb{R}^{(M - N_I + 1)}$, $i \in \{1, 2, \ldots, M - N_I + 1\}$, denotes the unit vector having only one nonzero entry at the ith position. The decimation matrix in (5) picks up data every D samples in a uniform manner. (If $D > B$, then the matrices $\boldsymbol{D}_k^{(b)}$ pick up different data from each other.) Although there are many other possibilities in the design of $\boldsymbol{D}_k^{(b)}$ presented in (5), the optimal decimation approach is clearly inefficient from a computational point of view as it results in extremely high computational complexity due to its combinatorial nature. In [13], it is shown that this simple design of matrices are effective in a block equalization application. The input signal to the reduced-rank adaptive FIR filter is given as

$$\widehat{\boldsymbol{u}}_k := \boldsymbol{D}_k \boldsymbol{V}_k^T \bar{\boldsymbol{u}}_k \in \mathbb{R}^P, \ \forall k \in \mathbb{N} \tag{6}$$

where

$$\bar{\boldsymbol{u}}_k := [u_k, u_{k-1}, \ldots, u_{k-M+1}]^T \in \mathbb{R}^M, \ \forall k \in \mathbb{N}. \tag{7}$$

Roughly speaking, $\boldsymbol{D}_k \boldsymbol{V}_k^T$ corresponds to the linear mapping $\boldsymbol{S}$; we emphasize that it changes dynamically in terms of k. Precisely speaking, if the dimension of $\bar{\boldsymbol{u}}_k$ is no greater than the dimension of $\boldsymbol{u}_k$, i.e., if $M \leq N$, then

$$\boldsymbol{S} = \boldsymbol{X} \boldsymbol{V}_k \boldsymbol{D}_k^T \tag{8}$$

where

$$\boldsymbol{X} := \left[\boldsymbol{I}_M \boldsymbol{O}_{M \times (N-M)} \right]^T \in \mathbb{R}^{N \times M}. \tag{9}$$

Here, $\boldsymbol{I}_n$ and $\boldsymbol{O}_{n \times m}$ denote the $n \times n$ identity matrix and the $n \times m$ zero matrix, respectively. When $M > N$, we need more data than $\boldsymbol{u}_k$ to represent $\bar{\boldsymbol{u}}_k$. The FIR filter output and the estimation error (residual error) are given as $y_k := \widehat{\boldsymbol{h}}_k^T \widehat{\boldsymbol{u}}_k$, $\forall k \in \mathbb{N}$, and $e_k := d_k - y_k$, $\forall k \in \mathbb{N}$, respectively.

B. Adaptive Algorithm

To derive an NLMS-based adaptive algorithm for two vectors $\boldsymbol{v}_k \in \mathbb{R}^{N_I}$ and $\widehat{\boldsymbol{h}}_k \in \mathbb{R}^P$, the following relation is useful:

$$y_k = \widehat{\boldsymbol{h}}_k^T \boldsymbol{D}_k \boldsymbol{U}_k^{(I)} \boldsymbol{v}_k = \widehat{\boldsymbol{h}}_k^T \boldsymbol{U}_k \boldsymbol{v}_k \tag{10}$$

where

$$\boldsymbol{U}_k^{(I)} := \begin{bmatrix} u_k & u_{k-1} & \cdots & u_{k-N_I+1} \\ \vdots & \vdots & \ddots & \vdots \\ u_{k-M+N_I} & u_{k-M+N_I-1} & \cdots & u_{k-M+1} \end{bmatrix} \in \mathbb{R}^{(M-N_I+1)\times N_I} \tag{11}$$

$$\boldsymbol{U}_k := \boldsymbol{D}_k \boldsymbol{U}_k^{(I)} \in \mathbb{R}^{P\times N_I}. \tag{12}$$

Note that y_k can be rewritten as $y_k(:= \widehat{\boldsymbol{h}}_k^T \widehat{\boldsymbol{u}}_k) = \boldsymbol{s}_k^T \boldsymbol{v}_k$, where $\boldsymbol{s}_k := \boldsymbol{U}_k^T \widehat{\boldsymbol{h}}_k \in \mathbb{R}^{N_I}$. We formulate the problem as follows:

$$\min_{(\boldsymbol{v},\widehat{\boldsymbol{h}})\in\mathbb{R}^{N_I}\times\mathbb{R}^P} \|\boldsymbol{v}_k - \boldsymbol{v}\|^2 + \left\|\widehat{\boldsymbol{h}}_k - \widehat{\boldsymbol{h}}\right\|^2 \quad \text{s.t. } \widehat{\boldsymbol{h}}_k^T \boldsymbol{U}_k \boldsymbol{v} = d_k \text{ and } \widehat{\boldsymbol{h}}^T \boldsymbol{U}_k \boldsymbol{v}_k = d_k. \tag{13}$$

Adopting the error minimization criterion for D_k, and noting that the problem in (13) is equivalent to finding the projections onto hyperplanes in $\mathbb{R}^{N_I}$ and $\mathbb{R}^P$, respectively for $\boldsymbol{v}$ and $\widehat{\boldsymbol{h}}$, we obtain the following equations [see Fig. 2(b)]:

$$\boldsymbol{v}_{k+1} = \boldsymbol{v}_k + \frac{\eta_k e_k \boldsymbol{s}_k}{\|\boldsymbol{s}_k\|^2} \tag{14}$$

$$\boldsymbol{D}_k = \boldsymbol{D}_k^{(b_k)} \text{ with } b_k := \arg \min_{b\in\{1,2,\ldots,B\}} |e_k^{(b)}| \tag{15}$$

$$\widehat{\boldsymbol{h}}_{k+1} = \widehat{\boldsymbol{h}}_k + \frac{\mu_k e_k \widehat{\boldsymbol{u}}_k}{\|\widehat{\boldsymbol{u}}_k\|^2} \tag{16}$$

where $e_k^{(b)} := d_k - \widehat{\boldsymbol{h}}_k^T \boldsymbol{D}_k^{(b)} \boldsymbol{V}_k^T \bar{\boldsymbol{u}}_k$, $\eta_k \in [0,2]$, and $\mu_k \in [0,2]$.

The proposed AEC scheme is summarized below.

1) $\widehat{\boldsymbol{u}}_k^{(b)} := \boldsymbol{D}_k^{(b)} \boldsymbol{V}_k^T \bar{\boldsymbol{u}}_k, \forall b \in \{1,2,\ldots,B\}$.
2) $e_k^{(b)} := d_k - \widehat{\boldsymbol{h}}_k^T \widehat{\boldsymbol{u}}_k^{(b)}, \forall b \in \{1,2,\ldots,B\}$.
3) $\boldsymbol{D}_k = \boldsymbol{D}_k^{(b_k)}$ with $b_k := \arg \min_{b\in\{1,2,\ldots,B\}} |e_k^{(b)}|$.
4) $\boldsymbol{s}_k = \left(\boldsymbol{D}_k \boldsymbol{U}_k^{(I)}\right)^T \widehat{\boldsymbol{h}}_k$, $\widehat{\boldsymbol{u}}_k = \widehat{\boldsymbol{u}}_k^{(b_k)}$, $e_k = e_k^{(b_k)}$.
5) $\boldsymbol{v}_{k+1} = \boldsymbol{v}_k + \eta_k e_k \boldsymbol{s}_k / \|\boldsymbol{s}_k\|^2$ with $\eta_k \in [0,2]$.
6) $\widehat{\boldsymbol{h}}_{k+1} = \widehat{\boldsymbol{h}}_k + \mu_k e_k \widehat{\boldsymbol{u}}_k / \|\widehat{\boldsymbol{u}}_k\|^2$ with $\mu_k \in [0,2]$.

The selective decimation in the step 3) and the adaptive interpolation in the step 5) are the key to improve the MSE performance, as demonstrated in Sections V and VI. In the steps 5) and 6), it is also possible to employ a more efficient algorithm such as the adaptive parallel subgradient projection (adaptive-PSP) algorithm [17] or its accelerated version [18]; the efficacy of the method in [18] has been demonstrated in the stereophonic AEC problem [19].

C. Computational Complexity

The computational complexity of the proposed reduced-rank scheme for AEC is treated in this part. Table I shows the computational complexity required by the proposed and conventional solutions, including the full-rank NLMS and RLS algorithms. The proposed reduced-rank structure introduces the term P, which denotes the dimension of the reduced-rank filter, the number of branches B, which are used for improving the estimation accuracy, and the decimation factor D. Indeed, the decimation factor D is central to significantly reduce the complexity of the overall scheme and should be chosen to be large enough. An example of the value of D corresponding to $P \in \{3,4,\ldots,20\}$ and $N = 1024$ is given in Table II. The diversity factor B should be sufficiently large to ensure that the projection by the matrix $\boldsymbol{S}$ is able to extract the key features of the input vector. In our studies, we noticed that the value D has no significant impact on the performance (a large D, e.g., $D = 300$ is sufficient) but a large B is extremely important to ensure a good and accurate feature extraction of the input data. A drawback of the MWF and AVF methods is that they require a complexity quadratic with N, which makes their adoption for the AEC problem an impediment.

TABLE I
COMPUTATIONAL COMPLEXITY OF ALGORITHMS

Algorithm	Number of operations per iteration	
	Additions	Multiplications
NLMS-Full-rank	$3N-1$	$3N+2$
NLMS-Proposed	$(N_I-1)\min\{BP, M-N_I+1\}$ $+N_I(P+1)+P(B+2)-2$	$N_I \min\{BP, M-N_I+1\}$ $+N_I(P+2)+P(B+2)$ $+B+3$
MWF-NLMS	$P[2(N-1)^2+N+3]$	$P(N^2+5N+7)$
RLS-Full-rank	$3(N-1)^2+N^2+2N$	$6N^2+2N+2$
MWF-RLS	$P[4(N-1)^2+2N]$	$P(4N^2+2N+3)$
AVF	$P[N^2+3(N-1)^2]$ $+P[5(N-1)+1]$ $+2(N-1)+1$	$P(4N^2+4N+1)$ $+4N+2$

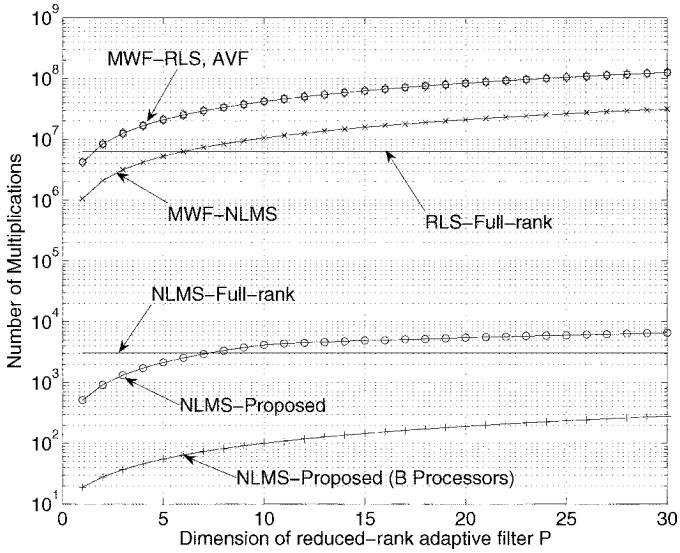

Fig. 3. Comparison of the computational complexity (number of multiplications) of the proposed and conventional methods.

Another interesting and unique aspect of the proposed scheme is that the computational burden of the algorithm can naturally be divided by B concurrent processors similarly to the adaptive-PSP based algorithms [17]–[19]. Fig. 3 plots the computational complexity (the number of multiplications) of each algorithm for $N = 1024$ with respect to the dimension of reduced-rank adaptive filter; for the proposed scheme, we assume that $B = 100$ and $N_I = 3$, as used in the following section. Note that the comparisons in the step 3) are assumed to require $B-1$ multiplications (due to storage similarly to multiplications). From the figure, it is seen that the total computational complexity of the proposed scheme for $P < 7$ is even less than that of the simple full-rank NLMS algorithm. In particular, for $P = 4$ (which is employed in the following

TABLE II
DECIMATION FACTOR D FOR EACH $P \in \{3, 4, \ldots, 20\}$

P	3	4	5	6	7	8	9	10	11	12	13	14	15	16	17	18	19	20
D	400	300	250	200	150	130	120	110	100	90	80	75	70	64	61	60	54	52

section) with B concurrent processors, the computational complexity imposed on each processor is approximately $0.045N$. We should mention that the proposed scheme has *fault tolerance nature* similarly to the methods in [17]–[19]. Namely, when some of the engaged processors get out of order during adaptation, we can discard the corresponding branches and utilize the other branches, thus such a trouble does *not* cause serious performance deterioration, as found in our studies.

We will finally discuss why the proposed scheme can achieve significant improvements of echo cancellation performance with such low computational costs. The complexity $0.045N$ shown above, corresponding to the lowest curves in Fig. 3, is a per-processor one, and can only be achieved when B parallel processors are available. Meanwhile, even in case that such parallel processors are not available, the computational complexity is $1.69N$, which is less than that of the simple full-rank NLMS algorithm. We emphasize that this complexity reduction is achieved by discarding an *unnecessary part* of input data and utilizing only the remaining part that contains the most important information to express the echo with the adaptive interpolator and FIR filter; this is also the key to realize significant improvements. Here, the " unnecessary part" refers to a portion of input data which has no significant contribution in expressing the echo. We remark that the proposed scheme can simply be implemented, and requires no extra hardware overloads compared to the conventional approaches.

D. Comparisons With Conventional AEC Techniques

One of the most popular AEC techniques is *the frequency-domain adaptive filtering (FDAF)* invented by Dentino *et al.* in 1978 [20]. Its major advantages over the time-domain adaptive filtering approach are faster convergence and lower computational complexity. However, the frequency-domain approach suffers in principle from block delay to perform the fast Fourier transform (FFT). A great deal of effort has been devoted to improve the performance of the FDAF, which is surveyed in [21] and [22]. In particular, *the multidelay block frequency domain (MDF) adaptive filter* using a small size FFT has been proposed by Soo and Pang in 1990 [23], which moderates the delay issue and achieves faster convergence and smaller memory requirements than the standard FDAF algorithm (a generalization has been done in [24]). Interesting modifications of the MDF method, based on the trigonometric transforms discrete cosine transform (DCT) and discrete sine transform (DST) and on the discrete Hartley transform (DHT), have been proposed in [25]. A delay-less frequency-domain algorithm has been proposed in [26], of which the performance is comparable to that of the full-band NLMS algorithm with computational complexity as low as the standard FDAF algorithms.

Another popular AEC technique is *the subband structure*, invented independently by Furukawa [27] and Kellermann [28] in 1984. The major advantages of the approach are its fast convergence in the initial phase of adaptation and low computational complexity. The subband approach, unfortunately, suffers from misalignment because 1) it is practically impossible to let the response in the stopband be completely zero, resulting in residual aliasing within the subband signals, and 2) the use of FIR filter introduces the truncation of the impulse responses [22]. Moreover, a major drawback of the approach is, similarly to the frequency-domain approach, the delay introduced in the analysis and synthesis filter banks (typically 20–40 ms for round-trip). To eliminate this issue, a delay-less subband adaptive filter, employing the polyphase FFT technique as a way of its implementation, has been proposed by Morgan and Thi in 1995 [29]. The delay-less subband technique has been analyzed in [30]–[32], and some modifications have been proposed in [33], [34]. Steady-state performance limitations of subband adaptive filters have been analyzed in [35].

The proposed scheme enjoys two unique advantages over the conventional techniques including the FDAF/subband and full-band approaches. One is the significant improvements in MSE due to *the selective decimation* and *the joint optimization of the adaptive interpolator and the FIR filter*, as described in the early part of this section (the achievable MSE is even less than those of the conventional techniques). The other is that its echo estimation error has a power spectrum uniformly distributing across the whole frequency band, which implies that the proposed scheme requires no echo suppressor unlike the conventional techniques (see Sections V and VI). Moreover, we mention that the proposed scheme causes no block delay, unlike the FDAF/subband approaches, because the scheme is based on sample-by-sample updates.

IV. CONVERGENCE PROPERTIES AND CONDITIONS

In this section, we discuss the global convergence of the proposed method and the convergence conditions in the form of the trajectory of the mean tap vectors. Specifically, we study the convergence properties of the proposed AEC scheme via the computation of the Hessian of the cost function.

A. Global Convergence of the Method and Its Properties

Let us describe the MMSE filter design of the proposed reduced-rank structure via the following cost function to be optimized:

$$J_{\mathrm{MSE}}(\widehat{\boldsymbol{h}}, \boldsymbol{v}) := E\Big[(d_k - \boldsymbol{v}^T \boldsymbol{U}_k^T \widehat{\boldsymbol{h}})^2\Big] \tag{17}$$

where $E[\cdot]$ stands for expectation. By fixing the interpolator $\boldsymbol{v} = \boldsymbol{v}_k \in \mathbb{R}^{N_I}$ and minimizing (17) with respect to $\widehat{\boldsymbol{h}} \in \mathbb{R}^P$, the suboptimal interpolated Wiener filter weight vector is

$$\widehat{\boldsymbol{h}}_k = \boldsymbol{\alpha}(\boldsymbol{v}_k) = \boldsymbol{R}_{\widehat{\boldsymbol{u}}}^{-1} \boldsymbol{p}_{\widehat{\boldsymbol{u}}} \tag{18}$$

where $\boldsymbol{R}_{\widehat{\boldsymbol{u}}} := E[\widehat{\boldsymbol{u}}_k\widehat{\boldsymbol{u}}_k^T]$, $\boldsymbol{p}_{\widehat{\boldsymbol{u}}} := E[d_k\widehat{\boldsymbol{u}}_k]$, $\widehat{\boldsymbol{u}}_k = \boldsymbol{U}_k\boldsymbol{v}_k$ and by fixing $\boldsymbol{h} = \widehat{\boldsymbol{h}}_k$ and minimizing (17) with respect to $\boldsymbol{v}$, the suboptimal interpolator weight vector is

$$\boldsymbol{v}_k = \boldsymbol{\beta}(\widehat{\boldsymbol{h}}_k) = \boldsymbol{R}_{\boldsymbol{s}}^{-1}\boldsymbol{p}_{\boldsymbol{s}} \tag{19}$$

where $\boldsymbol{R}_{\boldsymbol{s}} := E[\boldsymbol{s}_k\boldsymbol{s}_k^T]$, $\boldsymbol{p}_{\boldsymbol{s}} := E[d_k\boldsymbol{s}_k]$, and $\boldsymbol{s}_k = \boldsymbol{U}_k^T\widehat{\boldsymbol{h}}_k$. The associated MSE expressions are given as

$$J(\boldsymbol{v}) = J_{\mathrm{MSE}}(\boldsymbol{\alpha}(\boldsymbol{v}), \boldsymbol{v}) = \sigma_d^2 - \boldsymbol{p}_{\widehat{\boldsymbol{u}}}^T\boldsymbol{R}_{\widehat{\boldsymbol{u}}}^{-1}\boldsymbol{p}_{\widehat{\boldsymbol{u}}} \tag{20}$$

$$J_{\mathrm{MSE}}(\widehat{\boldsymbol{h}}, \boldsymbol{\beta}(\widehat{\boldsymbol{h}})) = \sigma_d^2 - \boldsymbol{p}_{\boldsymbol{s}}^T\boldsymbol{R}_{\boldsymbol{s}}^{-1}\boldsymbol{p}_{\boldsymbol{s}} \tag{21}$$

where $\sigma_d^2 := E[d_k^2]$. Note that points of global minimum of (17) can be obtained by $\boldsymbol{v}_{\mathrm{opt}} = \arg\min_{\boldsymbol{v}} J(\boldsymbol{v})$ and $\widehat{\boldsymbol{h}}_{\mathrm{opt}} = \boldsymbol{\alpha}(\boldsymbol{v}_{\mathrm{opt}})$ or $\widehat{\boldsymbol{h}}_{\mathrm{opt}} = \arg\min_{\widehat{\boldsymbol{h}}} J_{\mathrm{MSE}}(\widehat{\boldsymbol{h}}, \boldsymbol{\beta}(\widehat{\boldsymbol{h}}))$ and $\boldsymbol{v}_{\mathrm{opt}} = \boldsymbol{\beta}(\widehat{\boldsymbol{h}}_{\mathrm{opt}})$. At the minimum point, (20) coincides with (21) and the MMSE for the proposed structure is achieved. We remark that (18) and (19) are not closed-form solutions for $\widehat{\boldsymbol{h}}$ and $\boldsymbol{v}$ because (18) is a function of $\boldsymbol{v}$ and (19) depends on $\widehat{\boldsymbol{h}}$, and thus it is necessary to iterate adaptive recursions to estimate $\boldsymbol{v}_{\mathrm{opt}}$ and $\widehat{\boldsymbol{h}}_{\mathrm{opt}}$ with an initial guess.

We further note that, if $\boldsymbol{v}^\star$ is a global minimizer (a point achieving the global minimum) of $J(\boldsymbol{v})$, then $t\boldsymbol{v}^\star$ is also a global minimizer for any $t \neq 0$, since $J(\boldsymbol{v}) = J(t\boldsymbol{v})$. Therefore, we can assume without any loss of generality that $\|\boldsymbol{v}\| = 1$, and in this case global minimizers (optimum interpolator filters) can be obtained by $\boldsymbol{v}^\star = \arg\min_{\|\boldsymbol{v}\|=1} J(\boldsymbol{v})$. Since the existence of at least one global minimizer of the continuous function $J(\boldsymbol{v})$ for $\|\boldsymbol{v}\| = 1$ is guaranteed by the theorem of Weierstrass [36], then the existence of (infinitely many) global minimizers is also guaranteed for the cost function in (17). It should be mentioned that the global minimizers are invariant if the impulse response is invariant; this is exemplified in Section V-E, in which the filters converge to global minimizers.

In the context of global convergence, a sufficient but not necessary condition is *convexity* of the function J_{MSE}, which is verified if its Hessian matrix $\boldsymbol{H}$ is positive semi-definite; i.e., $\boldsymbol{a}^T\boldsymbol{H}\boldsymbol{a} \geq 0$, for any vector $\boldsymbol{a}$ in the space considered. First, let us consider the minimization, in terms of $\boldsymbol{v}$, of $J_{\mathrm{MSE}}(\widehat{\boldsymbol{h}}, \boldsymbol{v})$ in (17) with the FIR filter $\widehat{\boldsymbol{h}}$ fixed. The Hessian matrix is computed as

$$\boldsymbol{H} := \frac{\partial}{\partial \boldsymbol{v}^T}\frac{\partial J_{\mathrm{MSE}}(\cdot)}{\partial \boldsymbol{v}} = E\left[\widehat{\boldsymbol{u}}_k\widehat{\boldsymbol{u}}_k^T\right] = \boldsymbol{R}_{\widehat{\boldsymbol{u}}} \tag{22}$$

which is positive semi-definite, and thus ensures the convexity of the cost function in the case of fixed FIR filter.

Let us now consider the joint optimization of the interpolator $\boldsymbol{v}$ and the reduced-rank filter $\widehat{\boldsymbol{h}}$ through an equivalent cost function to (17):

$$\widetilde{J}_{\mathrm{MSE}}(\boldsymbol{z}) = E\left[(d_k - \boldsymbol{z}^T\boldsymbol{B}_k\boldsymbol{z})^2\right] \tag{23}$$

where $\boldsymbol{B}_k := \begin{bmatrix} \boldsymbol{O} & \boldsymbol{O} \\ \boldsymbol{U}_k^T & \boldsymbol{O} \end{bmatrix} \in \mathbb{R}^{(P+N_I)\times(P+N_I)}$ and $\boldsymbol{z} := \left[\widehat{\boldsymbol{h}}^T\ \boldsymbol{v}^T\right]^T \in \mathbb{R}^{(P+N_I)}$. In this case, the Hessian matrix $\widetilde{\boldsymbol{H}}$ with respect to $\boldsymbol{z}$ is given as

$$\widetilde{\boldsymbol{H}} := \frac{\partial}{\partial \boldsymbol{z}^T}\frac{\partial \widetilde{J}_{\mathrm{MSE}}(\cdot)}{\partial \boldsymbol{z}}$$

$$\begin{aligned} &= 2E\left[\left(\boldsymbol{B}_k + \boldsymbol{B}_k^T\right)\boldsymbol{z}\boldsymbol{z}^T\left(\boldsymbol{B}_k + \boldsymbol{B}_k^T\right)\right] \\ &\quad + 2E\left[\left(\boldsymbol{z}^T\boldsymbol{B}_k\boldsymbol{z} - d_k\right)\left(\boldsymbol{B}_k + \boldsymbol{B}_k^T\right)\right]. \end{aligned} \tag{24}$$

By examining $\widetilde{\boldsymbol{H}}$, we see that the first term is positive semidefinite, whereas the second one is indefinite. Hence, we cannot classify the optimization problem as convex. However, for a gradient-based algorithm, a desirable property of the cost function is that it has no points of local minimum, i.e., every point of minimum is a point of global minimum (convexity is a sufficient, but not necessary, condition for this property to hold) and our studies and experiments indicate that (23) has this property (see [37]). An important feature that advocates the nonexistence of local minima is that the algorithm always converges to the same minimum value, for a given experiment, independently of any interpolator initialization (except for $\boldsymbol{v}_0 = \boldsymbol{0}$ that eliminates the signal) for a wide range of signal-to-noise ratio (SNR) values and environments.

B. Convergence Conditions of the Algorithms

This part is devoted to the analysis of the trajectory of the mean tap vectors of the proposed AEC structure with the NLMS algorithm. In our analysis, we assume that the problem has no local minima and we employ the so-called independence theory [14]. To proceed, let us define the tap error vectors $\boldsymbol{e}_{\boldsymbol{v}_k}$ and $\boldsymbol{e}_{\widehat{\boldsymbol{h}}_k}$ as

$$\boldsymbol{e}_{\boldsymbol{v}_k} := \boldsymbol{v}_k - \boldsymbol{v}_{\mathrm{opt}},\ \boldsymbol{e}_{\widehat{\boldsymbol{h}}_k} := \widehat{\boldsymbol{h}}_k - \widehat{\boldsymbol{h}}_{\mathrm{opt}} \tag{25}$$

where $\widehat{\boldsymbol{h}}_{\mathrm{opt}}$ and $\boldsymbol{v}_{\mathrm{opt}}$ are the optimum tap vectors that achieve the MMSE for the proposed structure. By (14), (16), and (25), we can verify

$$\boldsymbol{e}_{\boldsymbol{v}_{k+1}} = \left[\boldsymbol{I} - \left(\frac{\eta_k}{\|\boldsymbol{s}_k\|^2}\right)\boldsymbol{s}_k\boldsymbol{s}_k^T\right]\boldsymbol{e}_{\boldsymbol{v}_k} + \left(\frac{\eta_k}{\|\boldsymbol{s}_k\|^2}\right)\boldsymbol{s}_k e_k^{v\mathrm{opt}} \tag{26}$$

$$\boldsymbol{e}_{\widehat{\boldsymbol{h}}_{k+1}} = \left[\boldsymbol{I} - \left(\frac{\mu_k}{\|\widehat{\boldsymbol{u}}_k\|^2}\right)\widehat{\boldsymbol{u}}_k\widehat{\boldsymbol{u}}_k^T\right]\boldsymbol{e}_{\widehat{\boldsymbol{h}}_k} + \left(\frac{\mu_k}{\|\widehat{\boldsymbol{u}}_k\|^2}\right)\widehat{\boldsymbol{u}}_k e_k^{h\mathrm{opt}} \tag{27}$$

where $e_k^{v\mathrm{opt}} := d_k - \boldsymbol{s}_k^T\boldsymbol{v}_{\mathrm{opt}}$ and $e_k^{h\mathrm{opt}} := d_k - \widehat{\boldsymbol{h}}_{\mathrm{opt}}^T\widehat{\boldsymbol{u}}_k$. By taking expectations on both sides, under the independence assumption, we have

$$E\left[\boldsymbol{e}_{\boldsymbol{v}_{k+1}}\right] = \left[\boldsymbol{I} - \widetilde{\eta}\boldsymbol{R}_{\boldsymbol{s}}\right]E\left[\boldsymbol{e}_{\boldsymbol{v}_k}\right] + \widetilde{\eta}E\left[\boldsymbol{s}_k e_k^{v\mathrm{opt}}\right] \tag{28}$$

$$E\left[\boldsymbol{e}_{\widehat{\boldsymbol{h}}_{k+1}}\right] = \left[\boldsymbol{I} - \widetilde{\mu}\boldsymbol{R}_{\widehat{\boldsymbol{u}}}\right]E\left[\boldsymbol{e}_{\widehat{\boldsymbol{h}}_k}\right] + \widetilde{\mu}E\left[\widehat{\boldsymbol{u}}_k e_k^{h\mathrm{opt}}\right] \tag{29}$$

where $\widetilde{\eta} := E\left[\eta_k/\|\boldsymbol{s}_k\|^2\right]$ and $\widetilde{\mu} := E\left[\mu_k/\|\widehat{\boldsymbol{u}}_k\|^2\right]$. We remark that the two error vectors have to be considered together because of the joint optimization of the interpolator filter and the reduced-rank filter. Rewriting the terms $E\left[\boldsymbol{s}_k e_k^{v\mathrm{opt}}\right]$ and $E\left[\widehat{\boldsymbol{u}}_k e_k^{h\mathrm{opt}}\right]$ with (25) and taking into account the independence theory [14], we obtain

$$\begin{aligned} E\left[\boldsymbol{s}_k e_k^{v\mathrm{opt}}\right] = &- E\left[\boldsymbol{s}_k\boldsymbol{v}_{\mathrm{opt}}^T\boldsymbol{U}_k^T\right]E\left[\boldsymbol{e}_{\widehat{\boldsymbol{h}}_k}\right] \\ &- E\left[\boldsymbol{s}_k\widehat{\boldsymbol{h}}_k^T\boldsymbol{U}_k\right]E\left[\boldsymbol{e}_{\boldsymbol{v}_k}\right] + \boldsymbol{p}_{\boldsymbol{s}} \\ &- E\left[\boldsymbol{s}_k\widehat{\boldsymbol{h}}_{\mathrm{opt}}^T\boldsymbol{U}_k\boldsymbol{v}_{\mathrm{opt}}\right] \end{aligned} \tag{30}$$

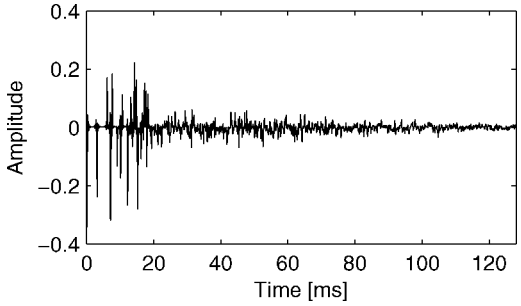

Fig. 4. The echo impulse response that is used in all the simulations.

$$E\left[\widehat{\boldsymbol{u}}_k e_k^{h\mathrm{opt}}\right] = -E\left[\widehat{\boldsymbol{u}}_k \widehat{\boldsymbol{h}}_{\mathrm{opt}}^T \boldsymbol{U}_k\right] E\left[\boldsymbol{e}_{\boldsymbol{v}_k}\right] - E\left[\widehat{\boldsymbol{u}}_k \boldsymbol{v}_k^T \boldsymbol{U}_k^T\right] E\left[\boldsymbol{e}_{\widehat{\boldsymbol{h}}_k}\right] + \boldsymbol{p}_{\widehat{\boldsymbol{u}}} - E\left[\widehat{\boldsymbol{u}}_k \widehat{\boldsymbol{h}}_{\mathrm{opt}}^T \boldsymbol{U}_k \boldsymbol{v}_{\mathrm{opt}}\right]. \quad (31)$$

By combining (28)–(31), the trajectory of the error vectors is given as

$$\begin{bmatrix} E\left[\boldsymbol{e}_{\boldsymbol{v}_{k+1}}\right] \\ E\left[\boldsymbol{e}_{\widehat{\boldsymbol{h}}_{k+1}}\right] \end{bmatrix} = \boldsymbol{A} \begin{bmatrix} E\left[\boldsymbol{e}_{\boldsymbol{v}_k}\right] \\ E\left[\boldsymbol{e}_{\widehat{\boldsymbol{h}}_k}\right] \end{bmatrix} + \boldsymbol{b} \quad (32)$$

where

$$\boldsymbol{A} := \begin{bmatrix} \boldsymbol{A}_{11} & \boldsymbol{A}_{12} \\ \boldsymbol{A}_{21} & \boldsymbol{A}_{22} \end{bmatrix} \quad (33)$$

$$\boldsymbol{b} := \begin{bmatrix} \widetilde{\eta}\left(\boldsymbol{p}_{\boldsymbol{s}} - E\left[\boldsymbol{s}_k \widehat{\boldsymbol{h}}_{\mathrm{opt}}^T \boldsymbol{U}_k \boldsymbol{v}_{\mathrm{opt}}\right]\right) \\ \widetilde{\mu}\left(\boldsymbol{p}_{\widehat{\boldsymbol{u}}} - E\left[\widehat{\boldsymbol{u}}_k \widehat{\boldsymbol{h}}_{\mathrm{opt}}^T \boldsymbol{U}_k \boldsymbol{v}_{\mathrm{opt}}\right]\right) \end{bmatrix} \quad (34)$$

$$\boldsymbol{A}_{11} := \boldsymbol{I} - \widetilde{\eta}\left\{\boldsymbol{R}_{\boldsymbol{s}} + E\left[\boldsymbol{s}_k \widehat{\boldsymbol{h}}_k^T \boldsymbol{U}_k\right]\right\} \quad (35)$$

$$\boldsymbol{A}_{12} := -\widetilde{\eta} E\left[\boldsymbol{s}_k \boldsymbol{v}_{\mathrm{opt}}^T \boldsymbol{U}_k^T\right] \quad (36)$$

$$\boldsymbol{A}_{21} := -\widetilde{\mu} E\left[\widehat{\boldsymbol{u}}_k \widehat{\boldsymbol{h}}_{\mathrm{opt}}^T \boldsymbol{U}_k\right] \quad (37)$$

$$\boldsymbol{A}_{22} := \boldsymbol{I} - \widetilde{\mu}\left\{\boldsymbol{R}_{\widehat{\boldsymbol{u}}} + E\left[\widehat{\boldsymbol{u}}_k \boldsymbol{v}_k^T \boldsymbol{U}_k^T\right]\right\}. \quad (38)$$

Equation (32) implies that the stability of the algorithms in the proposed structure depends on the matrix $\boldsymbol{A}$. For stability, the convergence factors should be chosen so that all the eigenvalues of $\boldsymbol{A}^T\boldsymbol{A}$ are less than unity. The simulations with the proposed scheme corroborate this analysis with respect to the tuning of step sizes.

V. Numerical Examples—Single-Talk Situations

In this section, we examine the performance of the proposed echo canceling scheme in single-talk situations; i.e., we assume $w_k = 0$, $\forall k \in \mathbb{N}$. We use a recorded speech input sampled at 8 kHz, an echo impulse response (see Fig. 4) recorded in a small room with its length 128 ms (i.e., $N = 1024$) and white noise with the signal to noise ratio (SNR) 10 dB, where the SNR is defined as $10\log_{10}(E\{z_k^2\}/E\{n_k^2\})$ with $z_k := \boldsymbol{u}_k^T\boldsymbol{h}^*(= d_k - n_k - w_k)$. The results are discussed in Section V-D.

A. Proposed Scheme With Different B and P

We investigate the performance of the proposed AEC scheme for different values of the diversity factor B and for different

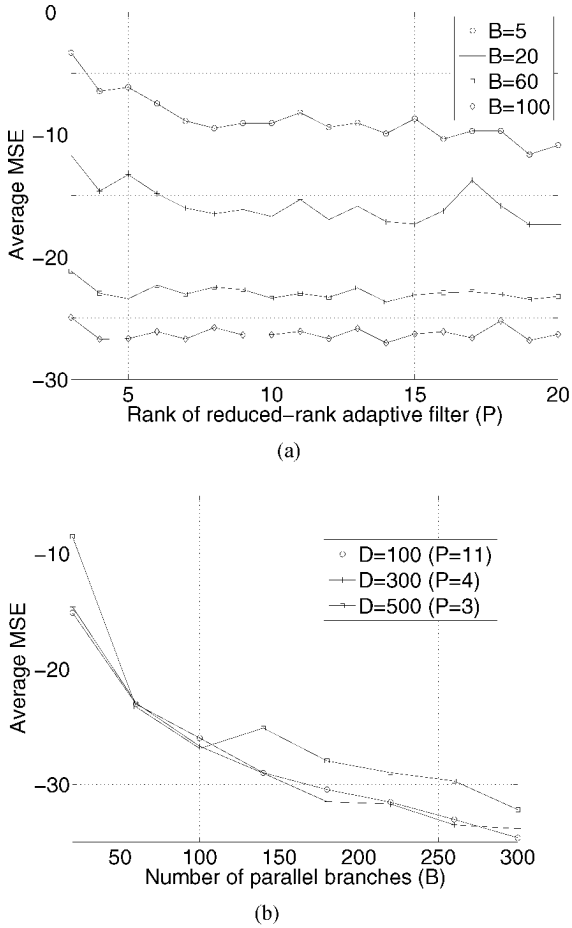

Fig. 5. Average MSE versus (a) rank of reduced-rank adaptive filter P and (b) number of parallel branches B.

ranks P of reduced-rank adaptive filter, which is dominated by the decimation factor D. For numerical stability against the poorly excited inputs, the algorithm is regularized with a factor $\delta = 0.01$ [14]. In the adaptation of $\boldsymbol{v}_k$ and $\widehat{\boldsymbol{h}}_k$, we employ $\mu_k = 0.4$, $\eta_k = 0.01$, $N_I = 3$, and $\boldsymbol{v}_0 = [0.5, 1.0, 0.5]^T$. The MSE at iteration k is defined as [38], [39]

$$\mathrm{MSE}(k) := \frac{\mathrm{LPF}\{(e_k - w_k)^2\}}{\mathrm{LPF}\{(d_k - w_k)^2\}},\ \forall k \in \mathbb{N} \quad (39)$$

where LPF denotes a low-pass filter with a single pole at 0.999 [38]; recall that $d_k := \boldsymbol{u}_k^T\boldsymbol{h}^* + w_k + n_k$ and $e_k = d_k - y_k$ for all $k \in \mathbb{N}$. We run 300 independent simulations; in each run, we average the MSE over 8000th to 10 000th iterations, and then average over 300 independent runs the averaged MSEs. Taking a careful look at (39), we see that the denominator will be small while the far-end speech is silent, whereas the numerator will be almost constant provided that the echo is reduced sufficiently. This means that, during silence, the MSE value will be increased even if the echo is canceled successfully. Hence, to avoid misleading, we use some small MSE values during the silent periods in all the experiments presented. The flat-periods in the MSE curves slightly longer than the silent periods and unstable-looking behavior (note: *not* unstable from system and filter theory points of view) observed in all the MSE figures are

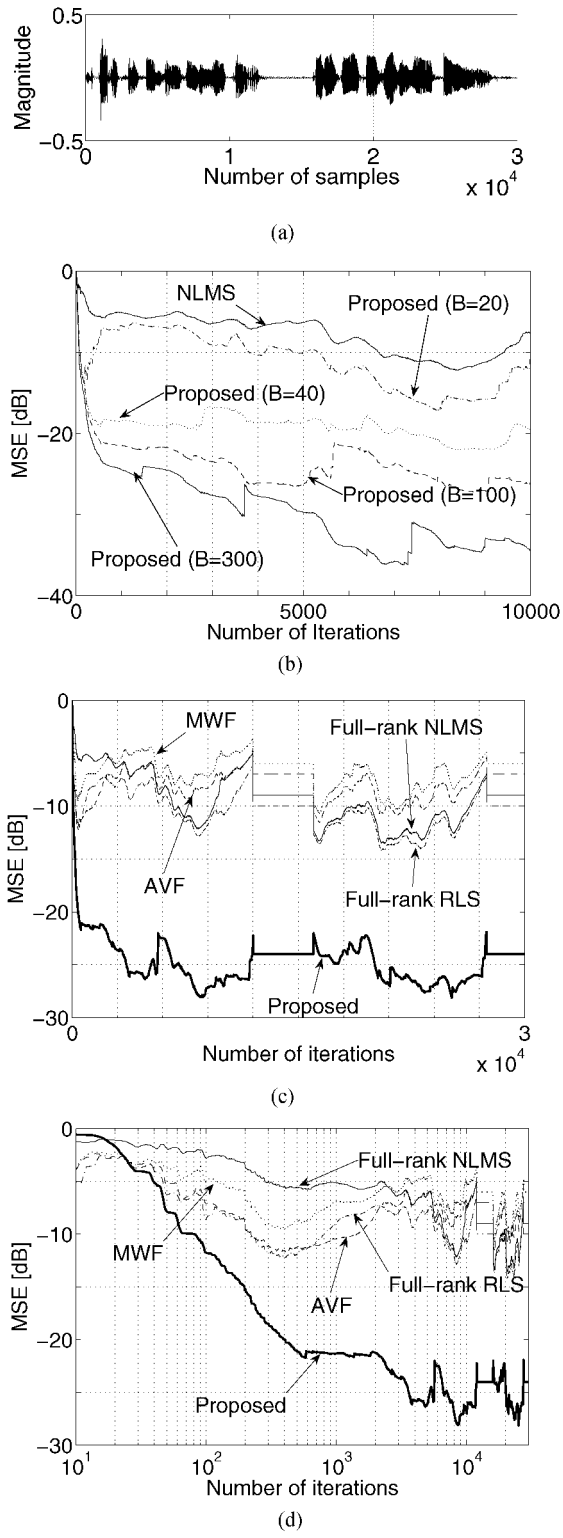

Fig. 6. (a) Input (far-end talker's) speech signal, (b) proposed schemes with different B versus NLMS; and proposed scheme versus the conventional algorithms with (c) linear and (d) logarithmic x-axes.

due to the low-pass filter, thus *never* being an essential problem (as supported by subjective tests in Section VI-B).

The results are drawn in Fig. 5. In Fig. 5(a), we set $B = 5$, 20, 60, and 100 and change P from 3 to 20. In Fig. 5(b), we set

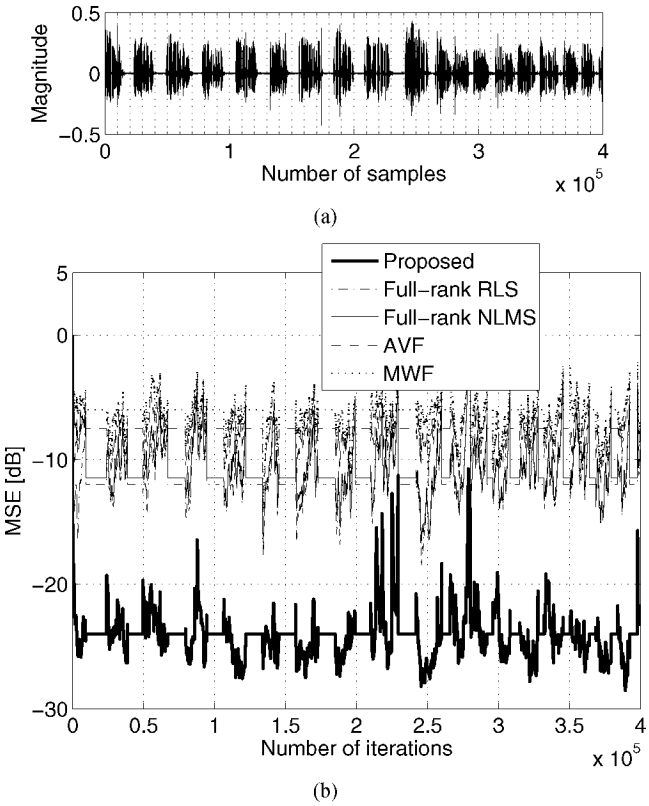

Fig. 7. (a) Input speech signal and (b) MSE curves.

$D = 100$, 300, 500, and $B = 20$, 60, 100, ..., 300. The speech signal employed in this section is depicted in Fig. 6(a).

B. Proposed Scheme Versus Conventional Schemes

We compare the convergence behavior of the proposed scheme with the NLMS algorithm to the full-rank NLMS, full-rank RLS, MWF, and AVF algorithms (note that the computational complexity of full-rank RLS, MWF, and AVF is prohibitively high as presented in Fig. 3). For the proposed scheme, we employ exactly the same parameters as in Fig. 5; $D = 300$ ($P = 4$) is selected [$B = 100$ in Fig. 6(c) and (d)]; in this case, the dimension of $\bar{\boldsymbol{u}}_k$ in (7) is $M\ [= B + D(P-1) + N_I - 1] = 1002\ (< 1024 = N)$. For the full-rank NLMS algorithm, we set $\mu = 0.1$. For the full-rank RLS algorithm, we use the forgetting factor $\lambda = 0.998$ (as it showed the best performance in our experiments), and the initial covariance matrix $\delta \boldsymbol{I}$ with $\delta = 0.1$. For the MWF algorithm, since the computational complexity to obtain the matrix tridiagonalizing the covariance matrix is prohibitively high, we use the following simple matrix [5]:

$$\boldsymbol{S}_k^{(\mathrm{MWF})} := [\boldsymbol{p}_k, \boldsymbol{R}_k\boldsymbol{p}_k, \ldots, \boldsymbol{R}_k^{P-1}\boldsymbol{p}_k] \in \mathbb{R}^{N\times P},\ \forall k \in \mathbb{N}$$

where $P = 4$, $\boldsymbol{R}_k := \lambda \boldsymbol{R}_{k-1} + \boldsymbol{u}_k\boldsymbol{u}_k^T$ and $\boldsymbol{p}_k := \lambda \boldsymbol{p}_{k-1} + d_k\boldsymbol{u}_k$ ($\lambda = 0.998$) with $\boldsymbol{R}_0 = \delta \boldsymbol{I}$ ($\delta = 0.1$) and $\boldsymbol{p}_0 = \boldsymbol{0}$. For the AVF algorithm, we use the following matrix [8]:

$$\boldsymbol{S}_k^{(\mathrm{AVF})} := [\boldsymbol{g}_1, \ldots, \boldsymbol{g}_P] \in \mathbb{R}^{N\times P},\ \forall k \in \mathbb{N}$$

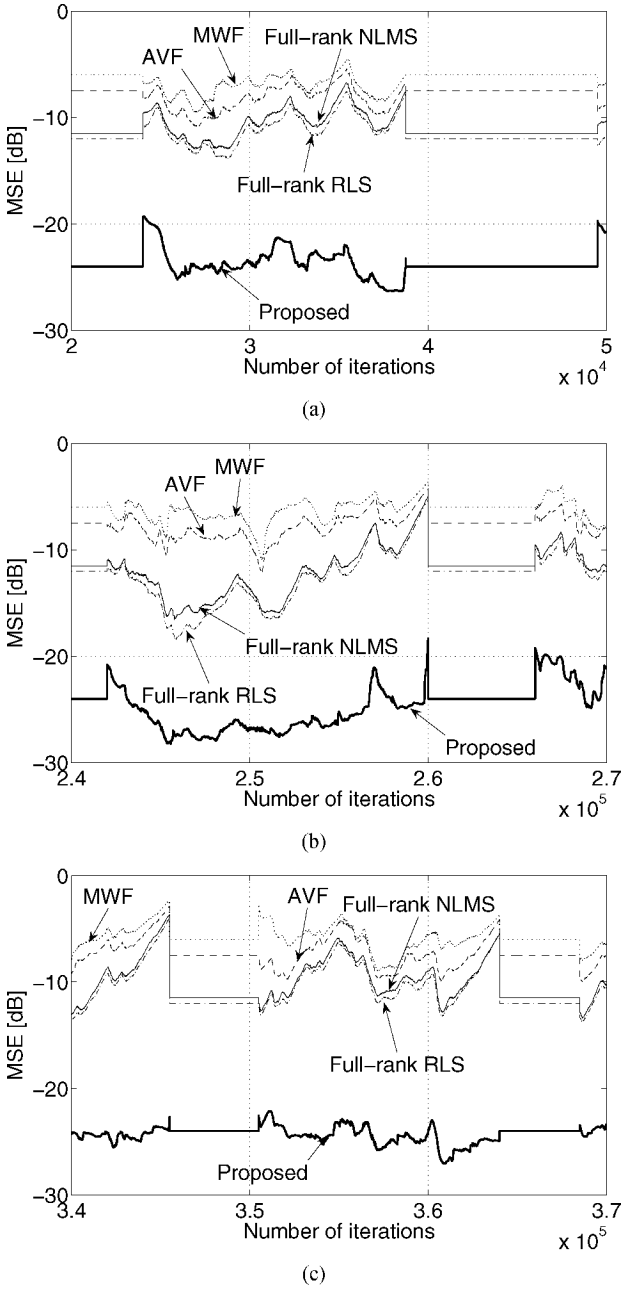

Fig. 8. MSE curves in (a) the early phase, (b) the intermediate phase, and (c) the late phase of adaptation.

where $P = 4$, $\boldsymbol{g}_1 = \boldsymbol{p}_k / \|\boldsymbol{p}_k\|$ and

$$\boldsymbol{g}_{i+1} = \frac{\boldsymbol{R}_k \boldsymbol{g}_i - \sum_{j=i-1}^{i} \boldsymbol{g}_j \left(\boldsymbol{g}_j^T \boldsymbol{R}_k \boldsymbol{g}_i\right)}{\left\| \boldsymbol{R}_k \boldsymbol{g}_i - \sum_{j=i-1}^{i} \boldsymbol{g}_j \left(\boldsymbol{g}_j^T \boldsymbol{R}_k \boldsymbol{g}_i\right) \right\|}, \quad i = 1, 2, \ldots, P-1.$$

The outputs of the MWF and AVF algorithms are, respectively, given as

$$y_k^{(\mathrm{MWF})} := \boldsymbol{u}_k^T \boldsymbol{S}_k^{(\mathrm{MWF})} \widehat{\boldsymbol{h}}_k^{(\mathrm{MWF})}, \ \forall k \in \mathbb{N} \tag{40}$$

$$y_k^{(\mathrm{AVF})} := \boldsymbol{u}_k^T \boldsymbol{S}_k^{(\mathrm{AVF})} \widehat{\boldsymbol{h}}_k^{(\mathrm{AVF})}, \ \forall k \in \mathbb{N}. \tag{41}$$

For the adaptation of the MWF reduced-rank adaptive filter $\widehat{\boldsymbol{h}}_k^{(\mathrm{MWF})}$, we adopt the NLMS algorithm with the step size $\mu_k = 0.4$ as in the proposed scheme. For the AVF scheme, since the weights $\widehat{\boldsymbol{h}}_k^{(\mathrm{AVF})} = [1, -c_1, -c_2, \ldots, -c_{P-1}]^T$ presented in [9] does not perform well due to the nonstationarity of speech, we instead employ the NLMS algorithm with the step size $\mu_k = 0.4$ to update the weights.

Fig. 6(b) draws the comparison among the proposed scheme with different values of diversity factor and the full-rank NLMS algorithm. Fig. 6(c) draws the comparison among the proposed scheme and the conventional algorithms. To clarify the behavior in the initial phase of adaptation, we adopt a logarithmic scale for the x-axis in Fig. 6(d).

C. Analysis of Echo Estimation Error

To demonstrate further the advantages of the proposed scheme, we perform another simulation with a larger number of speech samples, as depicted in Fig. 7(a). The employed algorithms and their parameters are exactly the same as in Fig. 6(c) and (d). The MSE curves are depicted in Fig. 7(b). To clarify how the behavior of each algorithm changes due to the progress of adaptation, we focus on three phases: (a) early phase 20 000–50 000, (b) intermediate phase 240 000–270 000, and (c) late phase 340 000–370 000; Fig. 8 depicts the MSE curves in each phase. Next, to examine how much the echo estimation error[2]

$$\varepsilon_k := \boldsymbol{u}_k^T \boldsymbol{h}^* - y_k \tag{42}$$

sounds similar to the original speech, we present their power spectrums. Fig. 9 depicts the power spectrum of the original signal $\boldsymbol{u}_k$ in each phase of adaptation; the power spectrums are respectively calculated over 10 000 samples as follows[3]: (a) 21 000–31000, (b) 245 000–255 000, and (c) 350 000–360 000. Fig. 10 depicts the power spectrum of the echo estimation error of the proposed, full-rank NLMS, MVF, and AVF algorithms in each phase. The power spectrums are calculated in the same way as the ones of the original speech.

D. Discussion for Single-Talk Case

From Fig. 5(a), we observe for $B = 5$, 20 significant improvements in the achievable MSE due to an increase of P, while negligible improvements for $B = 60$, 100. We see that, for a relatively large number of diversity factor (e.g., $B = 60$, 100), $P = 4$ is a reasonable choice. From Fig. 5(b), on the other hand, we see that an increase of B yields significant improvements. The diversity factor can be designed at user-requests.

Referring to Figs. 6–8, we see that the proposed algorithm with only four taps exhibits drastically faster convergence and even lower MSE in the steady state than the full-rank NLMS and RLS algorithms with 1024 taps. We stress again that the observed improvements in MSE come from the selective decimation and the adaptive interpolator. Moreover, an increase of

[2]This quantity is referred to as *undistorted error signal* in [40].

[3]The periods are selected so that the peak magnitude level is comparable among the three phases.

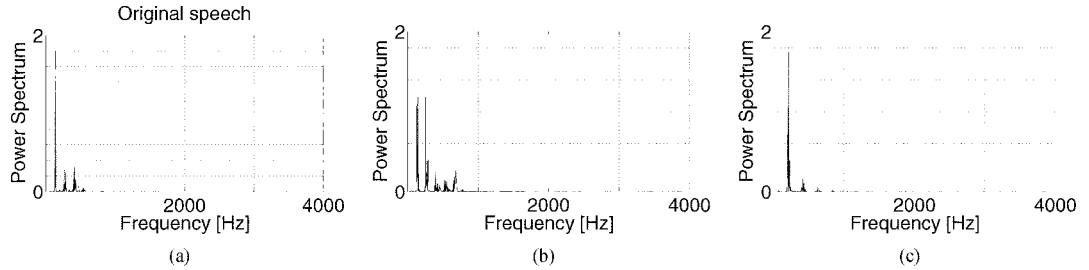

Fig. 9. Power spectrums of original speech in (a) the early phase, (b) the intermediate phase, and (c) the late phase of adaptation.

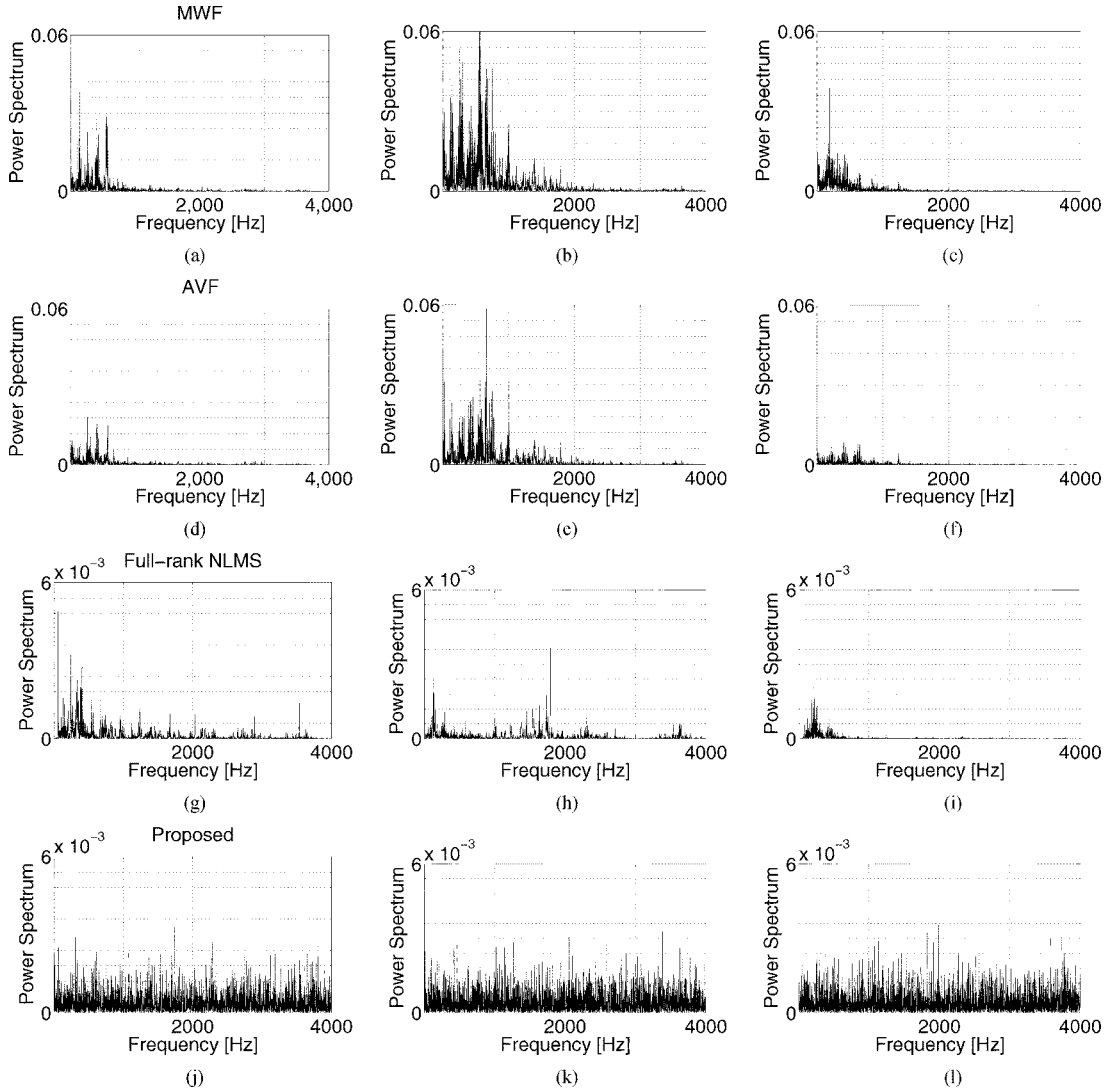

Fig. 10. (a)–(c) depict the power spectrums of echo estimation error for MWF in (a) the early phase, (b) the intermediate phase, and (c) the late phase of adaptation. In the same way, the figures (d)–(f) depict the ones for AVF, (g)–(i) the ones for full-rank NLMS, (j)–(l) the ones for the proposed method.

the diversity factor B improves the steady-state MSE performance by 10–15 dB compared to the full-rank NLMS and RLS algorithms without any loss in the initial speed of convergence.

From Fig. 10, we see that the power spectrum of the echo estimation error of the proposed scheme spreads over whole frequency, while the ones of NLMS, MWF, and AVF are concentrated in low frequency (as like the one of the original speech signal). This observation suggests that the residual echo of the proposed scheme performs as like noise unlike the ones of NLMS, MWF, and AVF; this is verified in our audio tests. As a result, the proposed scheme does not require an echo suppressor, which reduces the overall system complexity; we stress that this is *not* a common property of the reduced-rank filter *but* a unique property of the proposed scheme.

We remark that the total energy of the echo estimation error of the proposed scheme, which is directly related to echo return loss enhancement (ERLE) [15], could be more than that of the full-rank NLMS algorithm, as understood from Fig. 10. How-

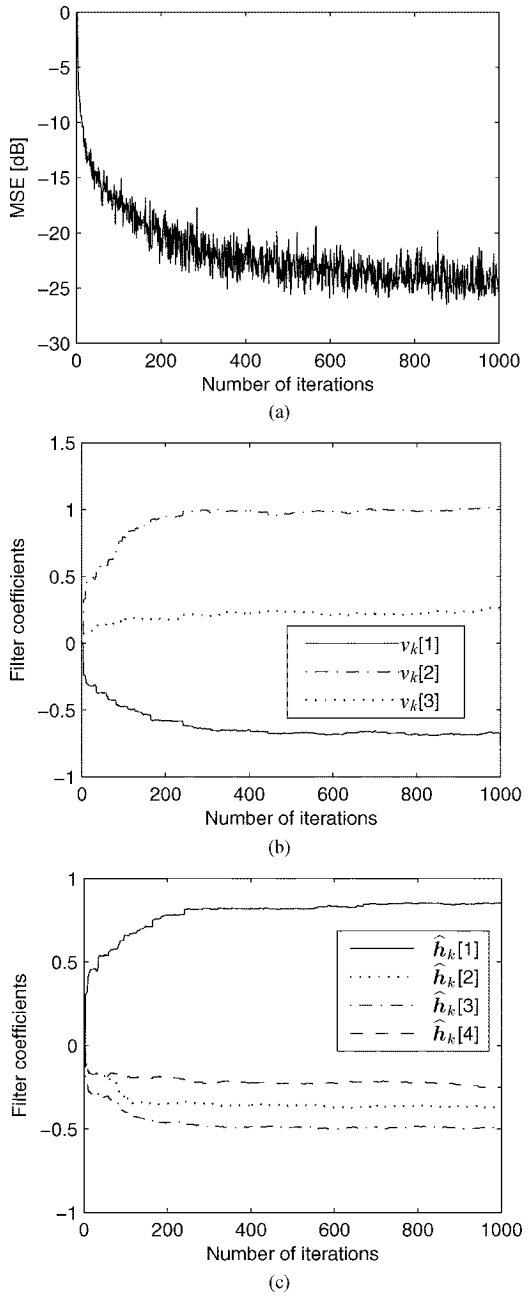

Fig. 11. (a) MSE curves, and the progress in time of (b) the interpolator $\boldsymbol{v}_k =: [v_k[1], v_k[2], v_k[3]]^T$, and (c) the FIR filter $\widehat{\boldsymbol{h}}_k =: [\widehat{h}_k[1], \widehat{h}_k[2], \widehat{h}_k[3], \widehat{h}_k[4]]^T$.

ever, the point is that the error of the proposed scheme has equal energy over whole frequency, and it is less annoying for human auditory perception than the error of the other methods, which will be verified by subjective assessment in Section VI-B. One may think that the residual error would be noisy, but it should be remarked that the residual error $d_k - y_k$ and the echo estimation error [see (42)] are different quantities and the energy of the former one is directly related to MSE. Therefore, the residual error of the proposed scheme is significantly small, as seen from Figs. 6–8. We thus provide no comparison in ERLE to avoid confusion.

E. Behavior of Interpolator and FIR Filter for White Input

Finally, we present the progress of the adaptive interpolator $\boldsymbol{v}_k$ and the FIR filter $\widehat{\boldsymbol{h}}_k$ for white input signals and how it decreases the MSE. To clarify the actions, we use the following definition (adopting no low-pass filter) rather than the one in (39):

$$\mathrm{MSE}(k) := \frac{\sum_{u=1}^{U}\left(e_k^{(u)} - w_k^{(u)}\right)^2}{\sum_{u=1}^{U}\left(d_k^{(u)} - w_k^{(u)}\right)^2},\ \forall k \in \mathbb{N} \tag{43}$$

which is an average over $U = 1000$ independent runs and $e_k^{(u)}$, $w_k^{(u)}$, and $d_k^{(u)}$ denote, respectively, e_k, w_k, and d_k at uth realization. The parameters and conditions are the same as in Section V-B. All coefficients of the vectors $\boldsymbol{v}_k \in \mathbb{R}^3$ and $\widehat{\boldsymbol{h}}_k \in \mathbb{R}^4$ are initialized to a random number close to zero with its variance 10^{-10}. The results are depicted in Fig. 11. Since the steady-state solution of $\boldsymbol{v}_k$ and $\widehat{\boldsymbol{h}}_k$ changes from a simulation to another, it makes no sense to take an average, and thus the filter coefficients shown in the figure are taken from one of the 1000 realizations; the behavior is nearly the same in all the realizations. In this example, the steady-state solution is approximately $\boldsymbol{v} = [-0.667, 1.01, 0.264]^T$ and $\widehat{\boldsymbol{h}} = [0.851, -0.370, -0.491, -0.2499]^T$.

In the simulation, we suppose that the impulse response of an echo path is time-invariant and the input signal is stationary, thus the steady-state solution of the two vectors is time-invariant. Otherwise, the algorithm can dynamically track an optimal solution. The key point is that we can model the reduced-rank filtering problem by introducing a projection matrix $\boldsymbol{S}$ [see (8)] that performs dimensionality reduction on the original data vector followed by a reduced-rank filter $\widehat{\boldsymbol{h}}_k$. In particular, the matrix $\boldsymbol{S}$ is a function of the interpolator $\boldsymbol{v}_k$ and the decimation matrix $\boldsymbol{D}_k$, which is time-varying and has a special structure, leading to a low-complexity scheme with extremely fast convergence and excellent tracking capability. In a situation where the proposed system reaches steady state, the filters can be frozen, and the decimation process can be halted provided the designer estimates $\boldsymbol{S}$. In such a case, the operation in steady state would only involve the dimensionality reduction of the original input data vector with $\boldsymbol{S}$ followed by filtering with the frozen coefficients of $\widehat{\boldsymbol{h}}_k$.

VI. Numerical Examples—Double-Talk Situations

In this section, we study the performance in double-talk situations; we concentrate here on the full-rank NLMS, full-rank RLS and proposed schemes. To cope with double-talk situations, we have two strategies:

1) construct a time-invariant $\boldsymbol{S}$ that can extract the key features of the input vector by means of the update information [e.g., $(\boldsymbol{D}_k)_{k\in\mathbb{N}}$ and $(\boldsymbol{v}_k)_{k\in\mathbb{N}}$];
2) develop an effective selection criterion working also in the double-talk situations to realize a time-variant $\boldsymbol{S}$.

The strategy 1) would be possible only if the system reaches steady state. In the current study, we focus on 2) and examine the potential of the proposed reduced-rank adaptive filtering scheme

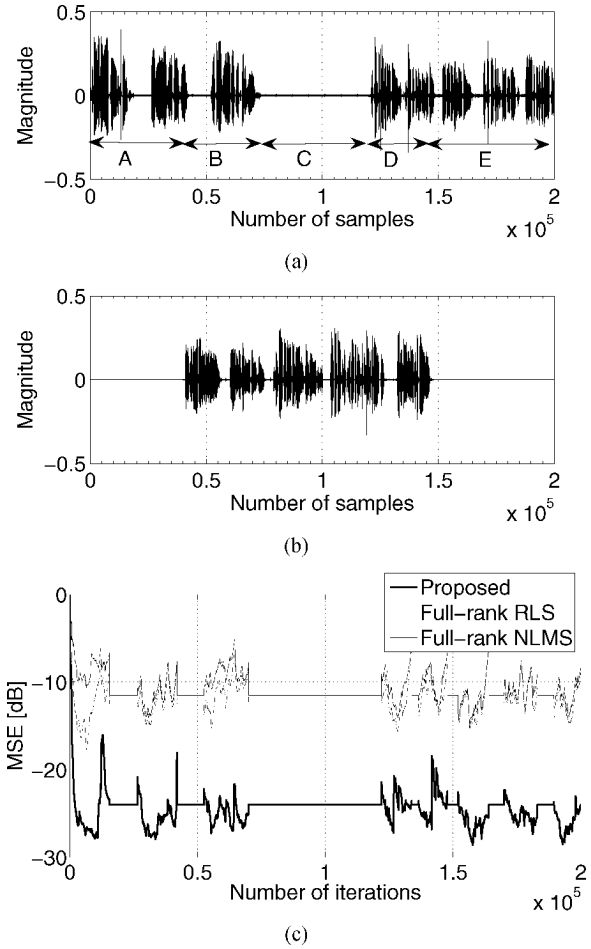

Fig. 12. (a) Far-end talker's speech signal. (b) Near-end talker's speech signal. (c) MSE curves.

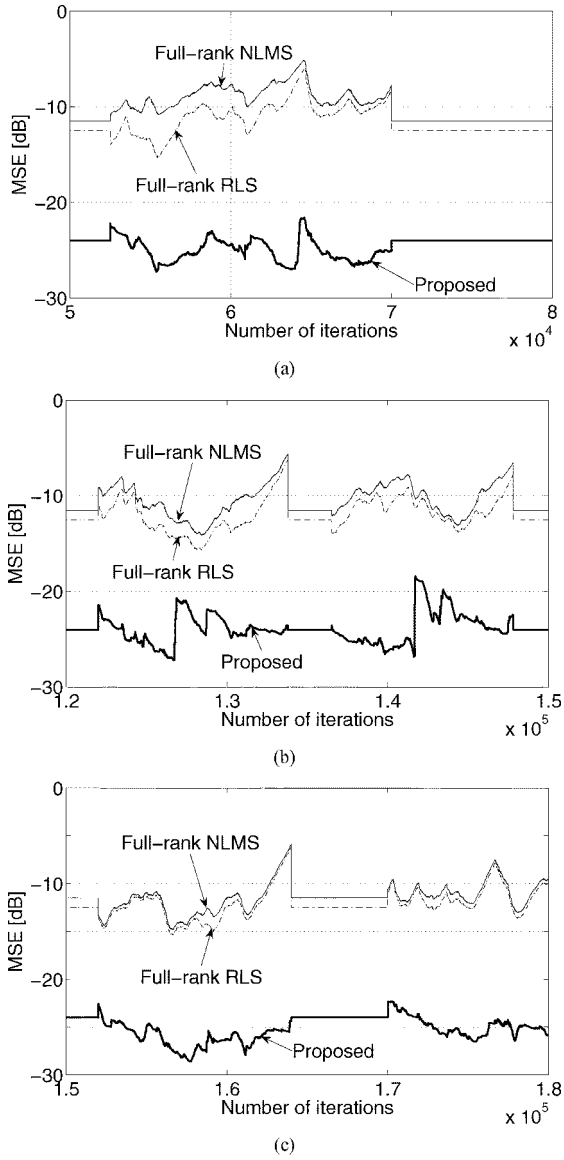

Fig. 13. MSE curves in a double-talk situation (a) in stage B, (b) in stage D, and (c) in stage E.

in the AEC problem with an ideal selection criterion; i.e., we assume that the filter selects the decimation matrix which minimizes $|e_k - w_k|, \forall k \in \mathbb{N}$. A cost-effective selection criterion for double-talk situations is an interesting open problem to be investigated in the future. For simplicity, we also assume for all the employed algorithms the perfect double-talk detection. For the proposed scheme, during the double-talk, we freeze the interpolator $\boldsymbol{v}_k$ and the FIR filter $\widehat{\boldsymbol{h}}_k$, while keeping the decimation matrix selection. For the full-rank NLMS and RLS schemes, during the double-talk, we freeze the updates of the filter coefficients; we keep updating the estimate of the autocorrelation matrix used in RLS whenever the far-end speech is active.

A. Comparisons in MSE and Power Spectrum

The employed far-end and near-end talker's speech is drawn in Fig. 12(a) and (b), respectively. Referring to both figures, we observe that the period is divided into five stages as depicted in Fig. 12(a): A) only far-end talker active, B) both far-end and near-end talkers active, C) only near-end talker active, D) both far-end and near-end talkers active as in the stage B, and (E) only far-end talker active as in the stage A. As the performance in the double-talk stages B and D and after-double-talk stage E are of our interest, we focus on three periods: (a) 50 000–80 000 in the stage B, (b) 120 000–150 000 in the stage D, and (c) 150 000–180 000 in the stage E. The employed parameters in each scheme are exactly the same as in Section V-C. Fig. 13 depicts the MSE in each period. The power spectrums are depicted in Fig. 14; the power spectrums in each period are respectively calculated over 10 000 samples as follows: (a) 55 000–65 000, (b) 125 000–135 000, and (c) 155 000–165 000. In addition to the objective evaluation, we present a subjective evaluation by means of listening tests in the following subsection.

B. Subjective Assessment

We conduct subjective tests to verify the advantage of the proposed scheme in a perceptive aspect over the full-rank NLMS algorithm. We prepare four pairs of near-end and far-end English speech samples, and each pair consists of (near-end speech, far-end speech) = (male, male), (male, female), (female, male), (female, female), respectively. After a training period (i.e., only far-end talker is active) for 5 s in which the adaptive filter is updated, we put a double-talk period for another 5 s in which

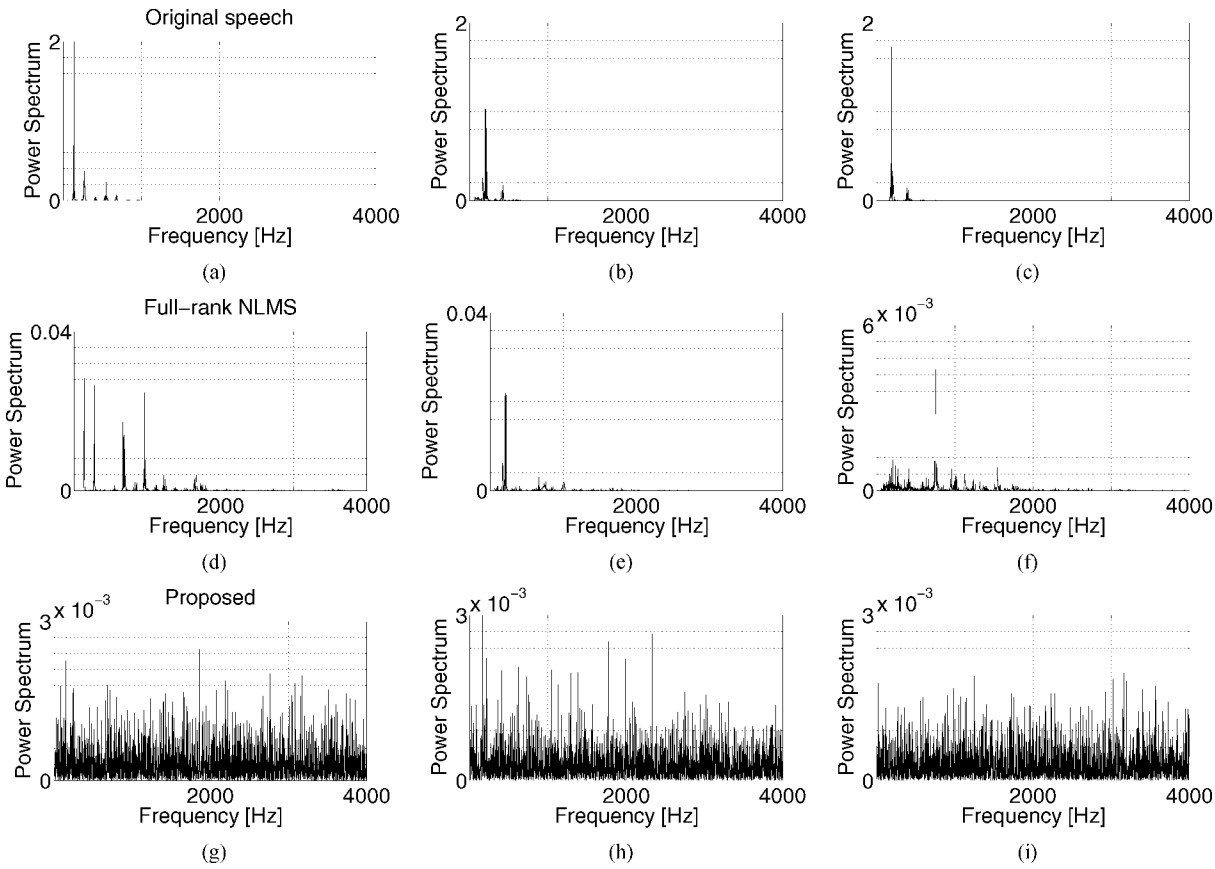

Fig. 14. (a)–(c) depict the power spectrums, in a double-talk case, of original speech in (a) the early phase, (b) the intermediate phase, and (c) the late phase of adaptation. In the same way, (d)–(f) depict the power spectrums of echo estimation error for full-rank NLMS, (g)–(i) the ones for the proposed method.

the adaptive filter is frozen and the far-end speech is canceled by the trained filter. We gather 25 English-native volunteers, including both male and female equally, with no knowledge about the current study for fairness. The volunteers listen to three types of speech, which are presented in a shuffled manner for unbiasedness: (a) the original (clean) near-end speech, (b) the one processed by the proposed scheme, and (c) the one processed by NLMS. The volunteers are asked to grade the quality of each speech according to the *absolute category rating* procedure [41] with a five grade scale: the minimum score is 1 corresponding to "bad" and the maximum is 5 corresponding to "excellent." Fig. 15 illustrates the results, where the vertical axis expresses mean opinion score (MOS), and the bar on each graph indicates the 99% confidence interval. It is seen that there is a significant difference between the proposed scheme and the full-rank NLMS algorithm.

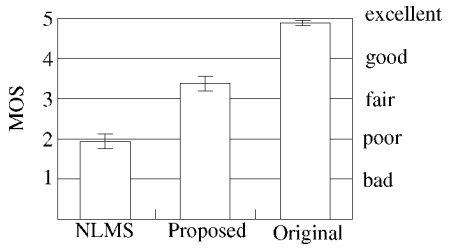

Fig. 15. MOS in the listening subjective tests. The bars indicate 99% confidence intervals.

C. Discussion for Double-Talk Case

From Figs. 12 and 13, we see that the proposed scheme substantially outperforms the full-rank methods all over the iterations. In particular, Fig. 13(c) demonstrates that the proposed scheme enjoys drastically fast tracking ability after the double-talk phases finish. Moreover, the results shown in the figures suggest that with an ideal criterion for decimation matrix selection the proposed scheme attains up to 15-dB gain in MSE compared to the full-rank approaches. Fig. 14 verifies that the echo estimation error of the proposed scheme in the double-talk situations spreads over whole frequency as in the single-talk situations. This implies a great benefit of the proposed scheme that the residual signal processed by the proposed scheme has no longer a characteristic of speech and thus the signal does not need to be postprocessed by echo suppressor any more unlike the conventional approaches. Fig. 15 verifies the advantage of the proposed scheme in human perception over the full-rank NLMS algorithm.

VII. Conclusion

This paper has proposed a new approach to an efficient echo cancellation based on reduced-rank adaptive filtering with adaptive interpolator and decimation-matrix-selection. The convergence properties of the proposed scheme and the convergence conditions have been discussed. The numerical examples have

demonstrated that the joint optimization approach will drastically improve the echo canceling ability with low computational complexity. This study has proven a substantial potential of the proposed approach. It would be an interesting future work to consider the strategies mentioned at the beginning of Section VI. From a wider point of view, this study has defined a new goal of efficient echo cancellation as finding a novel decimation selection criterion.

ACKNOWLEDGMENT

The authors would like to thank Dr. Y. Zakharov of the University of York for fruitful discussions. They would also like to thank all the volunteers involved in the subjective assessments for their warm hospitality. Finally, they would like to thank the anonymous reviewers for their invaluable comments on the original version of the manuscript.

REFERENCES

[1] A. M. Haimovich and Y. Bar-Ness, "An eigenanalysis interference canceler," *IEEE Trans. Signal Process.*, vol. 39, no. 1, pp. 76–84, Jan. 1991.

[2] Y. Song and S. Roy, "Blind adaptive reduced-rank detection for DS-CDMA signals in multipath channels," *IEEE J. Sel. Areas Commun.*, vol. 17, no. 11, pp. 1960–1970, Nov. 1999.

[3] J. S. Goldstein and I. S. Reed, "Reduced rank adaptive filtering," *IEEE Trans. Signal Process.*, vol. 45, no. 2, pp. 492–496, Feb. 1997.

[4] J. S. Goldstein, I. S. Reed, and L. L. Scharf, "A multistage representation of the Wiener filter based on orthogonal projections," *IEEE Trans. Signal Process.*, vol. 44, no. 11, pp. 2943–2959, Nov. 1998.

[5] M. L. Honig and J. S. Goldstein, "Adaptive reduced-rank interference suppression based on multistage Wiener filter," *IEEE Trans. Commun.*, vol. 50, no. 6, pp. 986–994, Jun. 2002.

[6] A. Kansal, S. N. Batalama, and D. A. Pados, "Adaptive maximum SINR RAKE filtering for DS-CDMA multipath fading channels," *IEEE J. Sel. Areas Commun.*, vol. 16, no. 9, pp. 1765–1773, Dec. 1998.

[7] H. Qian and S. N. Batalama, "Data record-based criteria for the selection of an auxiliary vector estimator of the MMSE/MVDR filter," *IEEE Trans. Commun.*, vol. 51, no. 10, pp. 1700–1708, Oct. 2003.

[8] W. Chen, U. Mitra, and P. Schniter, "On the equivalence of three reduced rank linear estimators with applications to DS-CDMA," *IEEE Trans. Inf. Theory*, vol. 48, no. 9, pp. 2609–2614, Sep. 2002.

[9] D. A. Pados and G. N. Karystinos, "An iterative algorithm for the computation of the MVDR filter," *IEEE Trans. Signal Process.*, vol. 49, no. 2, pp. 290–300, Feb. 2001.

[10] Y. Neuvo, D. Cheng-Yu, and S. K. Mitra, "Interpolated finite impulse response filters," *IEEE Trans. Acoust., Speech, Signal Process.*, vol. ASSP-32, no. 3, pp. 563–570, Jun. 1984.

[11] A. Abousaada, T. Aboulnasr, and W. Steenaart, "An echo tail canceller based on adaptive interpolated FIR filtering," *IEEE Trans. Circuits Syst.-II: Analog Digital Signal Process.*, vol. 39, no. 7, pp. 409–416, Jul. 1992.

[12] R. C. de Lamare and R. Sampaio-Neto, "Adaptive reduced-rank MMSE filtering with interpolated FIR filters and adaptive interpolators," *IEEE Signal Process. Lett.*, vol. 12, no. 3, pp. 177–180, Mar. 2005.

[13] R. C. de Lamare and R. Sampaio-Neto, "Adaptive reduced-rank MMSE parameter estimation based on an adaptive diversity combined decimation and interpolation scheme," in *Proc. IEEE ICASSP*, 2007, pp. 1317–1320.

[14] S. Haykin, *Adaptive Filter Theory*, 4th ed. Upper Saddle River, New Jersey: Prentice-Hall, 2002.

[15] C. Breining, P. Dreiseitel, E. Hänsler, A. Mader, B. Nitsch, H. Puder, T. Schertler, G. Schmidt, and J. Tilp, "Acoustic echo control —An application of very-high-order adaptive filters," *Signal Process. Mag.*, vol. 16, no. 4, pp. 42–69, Jul. 1999.

[16] S. L. Gay and J. Benesty, Eds., *Acoustic Signal Processing for Telecommunication*. Norwell, MA: Kluwer, 2000.

[17] I. Yamada, K. Slavakis, and K. Yamada, "An efficient robust adaptive filtering algorithm based on parallel subgradient projection techniques," *IEEE Trans. Signal Process.*, vol. 50, no. 5, pp. 1091–1101, May 2002.

[18] M. Yukawa and I. Yamada, "Pairwise optimal weight realization—Acceleration technique for set-theoretic adaptive parallel subgradient projection algorithm," *IEEE Trans. Signal Process.*, vol. 54, no. 12, pp. 4557–4571, Dec. 2006.

[19] M. Yukawa, N. Murakoshi, and I. Yamada, "Efficient fast stereo acoustic echo cancellation based on pairwise optimal weight realization technique," *EURASIP J. Appl. Signal Process.*, vol. 2006, 2006, paper 84797.

[20] M. Dentino, J. McCool, and B. Widrow, "Adaptive filtering in the frequency domain," *Proc. IEEE*, vol. 66, no. 12, pp. 1658–1659, Dec. 1978.

[21] J. J. Shynk, "Frequency-domain and multirate adaptive filtering," *IEEE Signal Process. Mag.*, vol. 9, no. 1, pp. 14–39, Jan. 1992.

[22] J. Benesty, T. Gänsler, D. R. Morgan, M. M. Sondhi, and S. L. Gay, *Advances in Network and Acoustic Echo Cancellation*. Berlin, Germany: Springer-Verlag, 2001.

[23] J.-S. Soo and K. K. Pang, "Multidelay block frequency domain adaptive filter," *IEEE Trans. Acoust., Speech, Signal Process.*, vol. 38, no. 2, pp. 373–376, Feb. 1990.

[24] E. Moulines, O. A. Amrane, and Y. Grenier, "The generalized multidelay adaptive filter: Structure and convergence analysis," *IEEE Trans. Signal Process.*, vol. 43, no. 1, pp. 14–28, Jan. 1995.

[25] R. Merched and A. H. Sayed, "An embedding approach to frequency-domain and subband adaptive filtering," *IEEE Trans. Signal Process.*, vol. 48, no. 9, pp. 2607–2619, Sep. 2000.

[26] Y. Bendel, D. Burshtein, O. Shalvi, and R. Weinstein, "Delayless frequency domain acoustic echo cancellation," *IEEE Trans. Speech Audio Process.*, vol. 9, no. 5, pp. 589–597, Jul. 2001.

[27] I. Furukawa, "A design of canceller of broad band acoustic echo," in *Proc. Int. Teleconf. Symp.*, 1984, pp. 1/8–8/8.

[28] W. Kellermann, "Kompensation akustischer echos in frequenzteil-bändern," in *Proc. Aachener Kolloquium*, 1984, pp. 322–325.

[29] D. R. Morgan and J. C. Thi, "A delayless subband adaptive filter architecture," *IEEE Trans. Signal Process.*, vol. 43, no. 8, pp. 1819–1830, Aug. 1995.

[30] N. Hirayama and H. Sakai, "Analysis of a delayless subband adaptive filter," in *Proc. IEEE ICASSP*, 1997, pp. 2329–2332.

[31] P. S. R. Diniz, R. Merched, and M. R. Petraglia, "Analysis of a delayless subband adaptive filter structure," in *Proc. IEEE ICASSP*, 1998, pp. 1661–1664.

[32] S. Ohno and H. Sakai, "On delayless subband adaptive filtering by subband/fullband transforms," *IEEE Signal Process. Lett.*, vol. 6, no. 9, pp. 236–239, Sep. 1999.

[33] R. Merched, P. S. R. Diniz, and M. R. Petraglia, "A new delayless subband adaptive filter structure," *IEEE Trans. Signal Process.*, vol. 47, no. 6, pp. 1580–1591, Jun. 1999.

[34] N. Hirayama, H. Sakai, and S. Miyagi, "Delayless subband adaptive filtering using the Hadamard transform," *IEEE Trans. Signal Process.*, vol. 47, no. 6, pp. 1731–1734, Jun. 1999.

[35] S. Weiss, A. S. R. W. Stewart, and R. Rabenstein, "Steady-state performance limitations of subband adaptive filters," *IEEE Trans. Signal Process.*, vol. 49, no. 9, pp. 1982–1991, Sep. 2001.

[36] D. P. Bertsekas, *Nonlinear Programming*, 2nd ed. Nashua, NH: Athena Scientific, 1999.

[37] R. C. de Lamare and R. Sampaio-Neto, "Adaptive interference suppression for DS-CDMA systems based on interpolated FIR filters with adaptive interpolators in multipath channels," *IEEE Trans. Veh. Technol.*, vol. 56, no. 5, pp. 2457–2474, Sep. 2007.

[38] T. Gänsler, S. L. Gay, M. M. Sondhi, and J. Benesty, "Double-talk robust fast converging algorithms for network echo cancellation," *IEEE Trans. Speech Audio Process.*, vol. 8, no. 6, pp. 656–663, Nov. 2000.

[39] Y. Huang and J. Benesty, Eds., *Audio Signal Processing for Next-Generation Multimedia Communication Systems*. Norwell, MA: Kluwer, 2004.

[40] E. Hänsler and G. Schmidt, *Acoustic Echo and Noise Control —A Practical Approach*. New York: Wiley, 2004.

[41] "Methods for subjective determination of transmission quality," 1996.

Masahiro Yukawa (S'05–M'06) received the B.E., M.E., and Ph.D. degrees from the Tokyo Institute of Technology, Tokyo, Japan, in 2002, 2004, and 2006, respectively.

From April 2005 to March 2007, he was a Research Fellow of the Japan Society for the Promotion of Science (JSPS). He spent the last six months of the fellowship as a Postdoctoral Fellow at the University of York, York, U.K. He is currently a Special Postdoctoral Researcher in the Next Generation Mobile Communications Laboratory, RIKEN, Saitama, Japan. His research interests include mathematical adaptive signal processing with applications to acoustic/communication systems.

Dr. Yukawa is a member of the Institute of Electrical, Information and Communication Engineers (IEICE) of Japan. He received the Excellent Paper Award from the IEICE in 2006 and the Yasujiro Niwa Outstanding Paper Award from Tokyo Denki University in 2007.

Rodrigo C. de Lamare (S'99–M'04) received the Diploma in electronic engineering from the Federal University of Rio de Janeiro (UFRJ), Rio de Janeiro, Brazil, in 1998 and the M.Sc. and Ph.D. degrees in electrical engineering from the Pontifical Catholic University of Rio de Janeiro (PUC-Rio) in 2001 and 2004, respectively.

From January 2004 to June 2005, he was a Postdoctoral Fellow at the Center for Studies in Telecommunications (CETUC), PUC-Rio, and from July 2005 to January 2006, he worked as a Postdoctoral Fellow at the Signal Processing Laboratory, UFRJ. Since January 2006, he has been with the Communications Research Group, Department of Electronics, University of York, York, U.K., where he is currently a Lecturer in Communications Engineering. His research interests lie in communications and signal processing.

Raimundo Sampaio-Neto received the Diploma and M.Sc. degrees both in electrical engineering from Pontifical Catholic University of Rio de Janeiro (PUC-Rio), Rio de Janeiro, Brazil, in 1975 and 1978, respectively, and the Ph.D. degree in electrical engineering from the University of Southern California (USC), Los Angeles, in 1983.

From 1978 to 1979, he was an Assistant Professor at PUC-Rio, and from 1979 to 1983, he was a doctoral student and a Research Assistant in the Department of Electrical Engineering at USC with a fellowship from CAPES. From November 1983 to June 1984, he was a Postdoctoral Fellow at the Communication Sciences Institute, Department of Electrical Engineering, USC, and a member of the technical staff of Axiomatic Corporation, Los Angeles. He is now a Researcher at the Center for Studies in Telecommunications (CETUC) and an Associate Professor of the Department of Electrical Engineering, PUC-Rio, where he has been since July 1984. During 1991, he was a Visiting Professor in the Department of Electrical Engineering at USC. He has participated in various projects and has consulted for several private companies and government agencies. He was co-organizer of the Session on Recent Results for the IEEE Workshop on Information Theory, 1992, Salvador. He has also served as Technical Program co-Chairman for IEEE Global Telecommunications Conference (Globecom'99) held in Rio de Janeiro in December 1999 and as a member of the technical program committees of several national and international conferences. He was in office for two consecutive terms for the Board of Directors of the Brazilian Communications Society where he is now a member of its Advisory Council and Associate Editor of the *Journal of the Brazilian Communication Society*. His areas of interest include communication systems theory, digital transmission, satellite communications, and signal processing for communications.